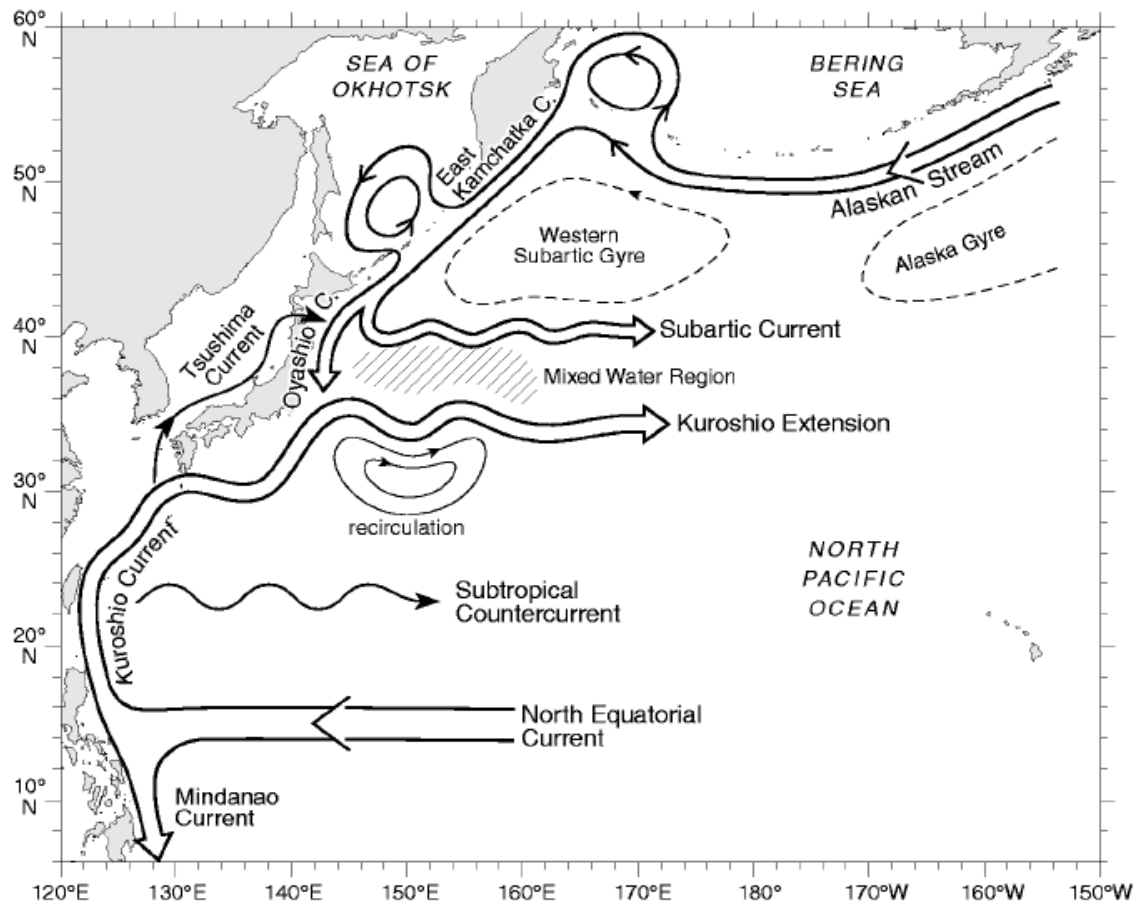


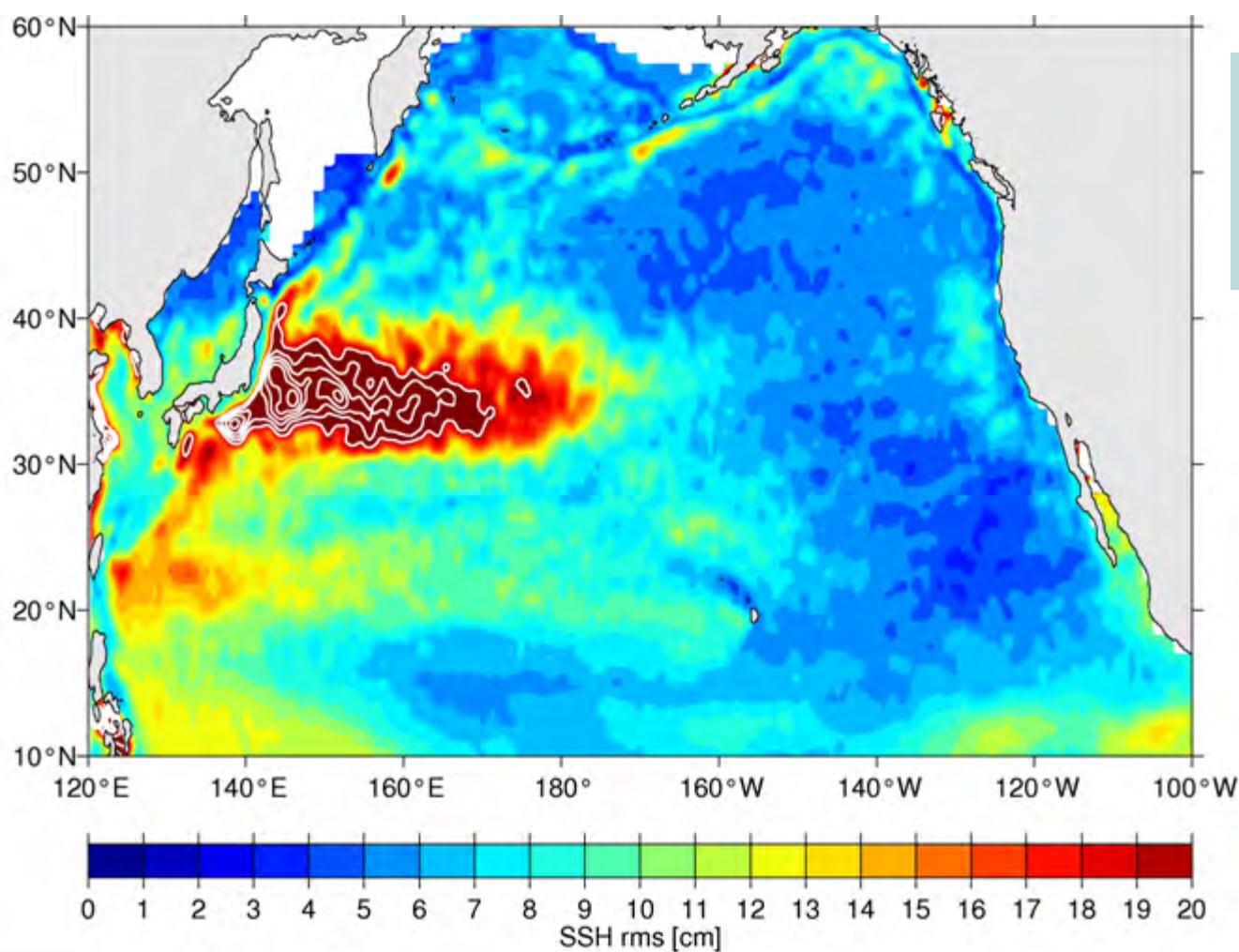
Forced vs Intrinsic Variability of the Kuroshio Extension System on Decadal Timescales

B. Qiu, S. Chen, and N. Schneider

Dept of Oceanography, University of Hawaii at Manoa



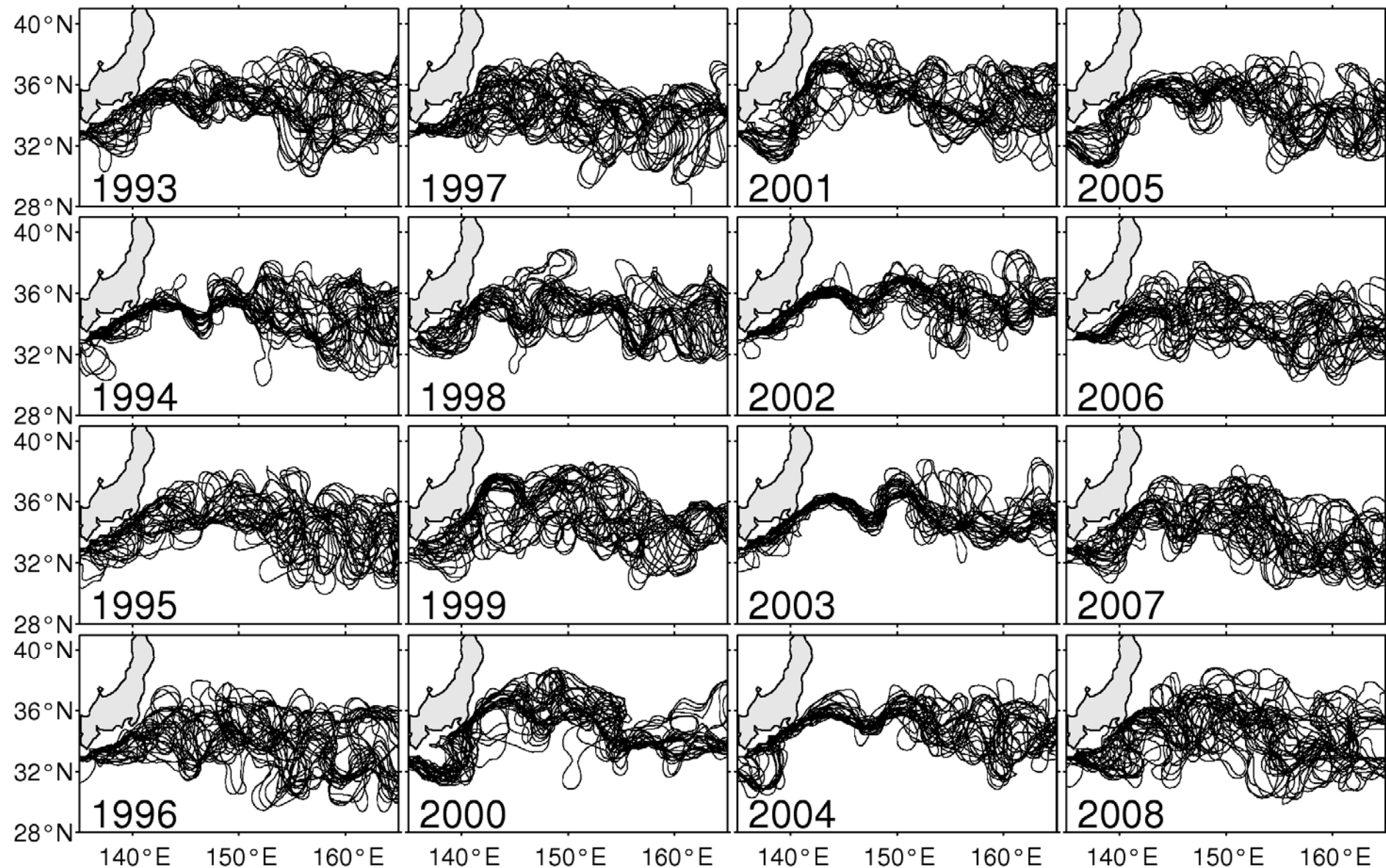
Satellite altimeter-derived rms SSH variability (10/1992-present)



Topics

- Observed decadally-varying KE system
- Relative roles of wind forcing vs nonlinear eddy dynamics
- Decadal KE variability as a midlatitude coupled mode

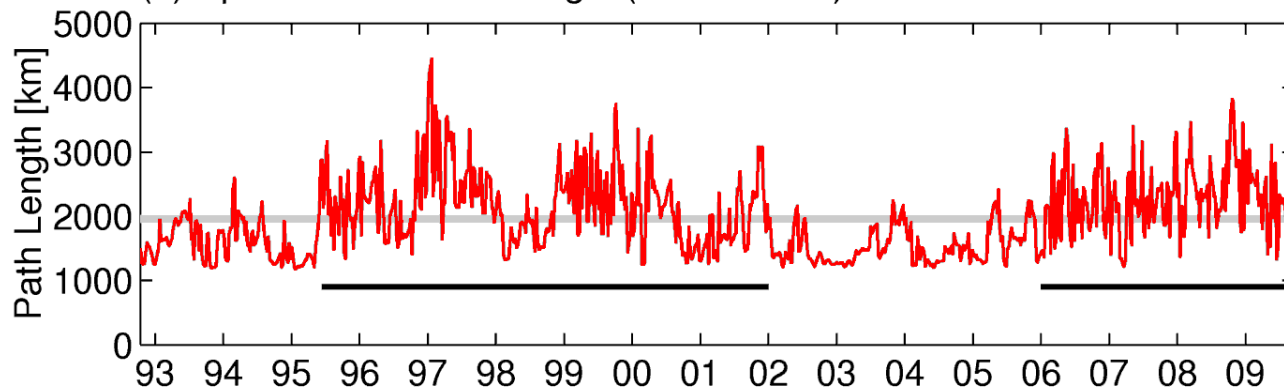
Semi-monthly Kuroshio Extension paths (1.7m SSH contours)



Stable yrs: 1993-94, 2002-04

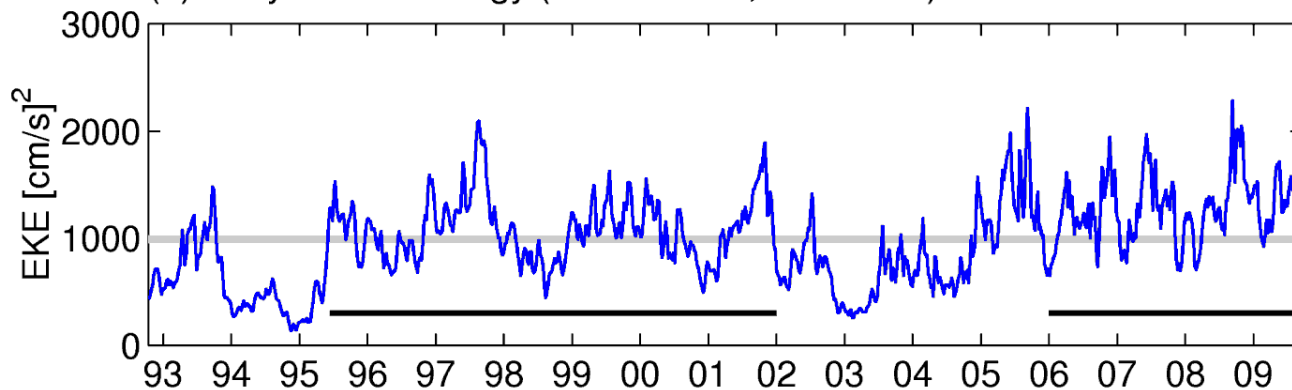
Unstable yrs: 1996-2001, 2006-08

(a) Upstream KE Path Length (141°–153°E)



KE path length

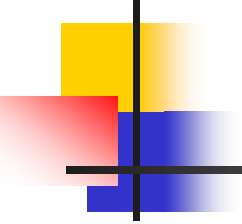
(b) Eddy Kinetic Energy (141°–153°E, 32°–38°N)



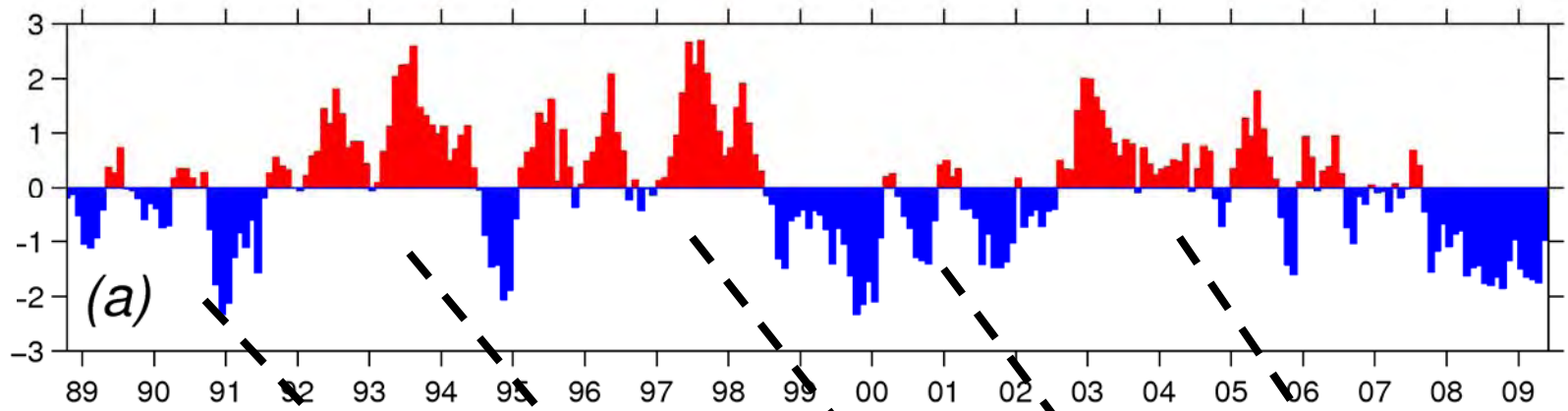
Level of EKE

Stable yrs: 1993-94, 2002-04

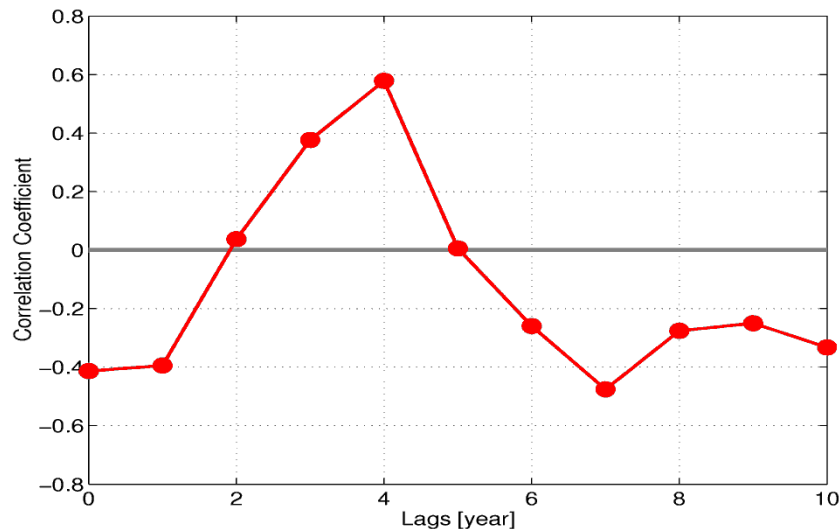
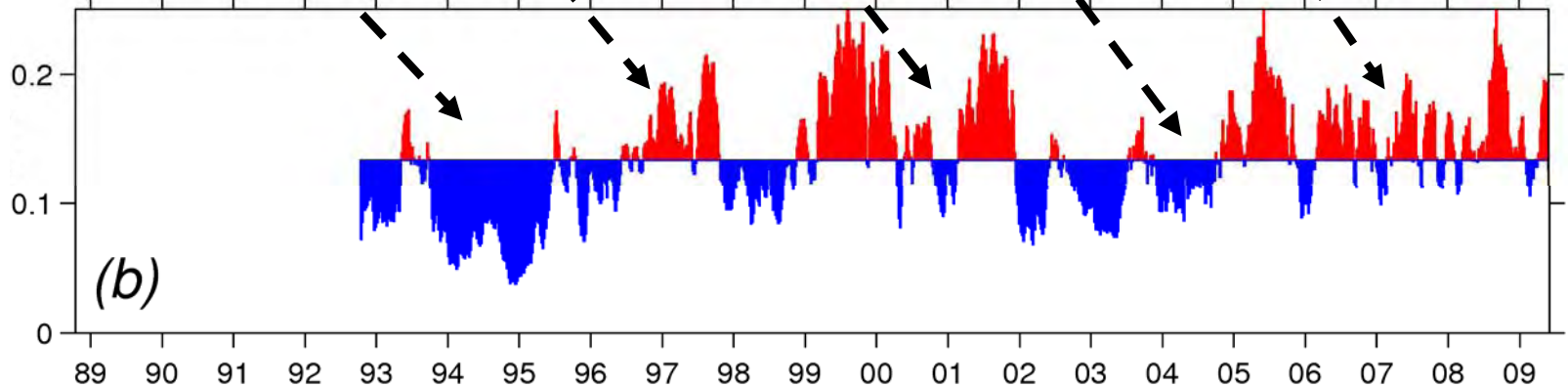
Unstable yrs: 1996-2001, 2006-08

- 
-
- **Q1: What causes the transitions between the stable and unstable dynamic states of the KE system?**

**PDO
index**



**EKE
level**



Mesoscale EKE level in the KE region lags the PDO index by ~ 4 yrs

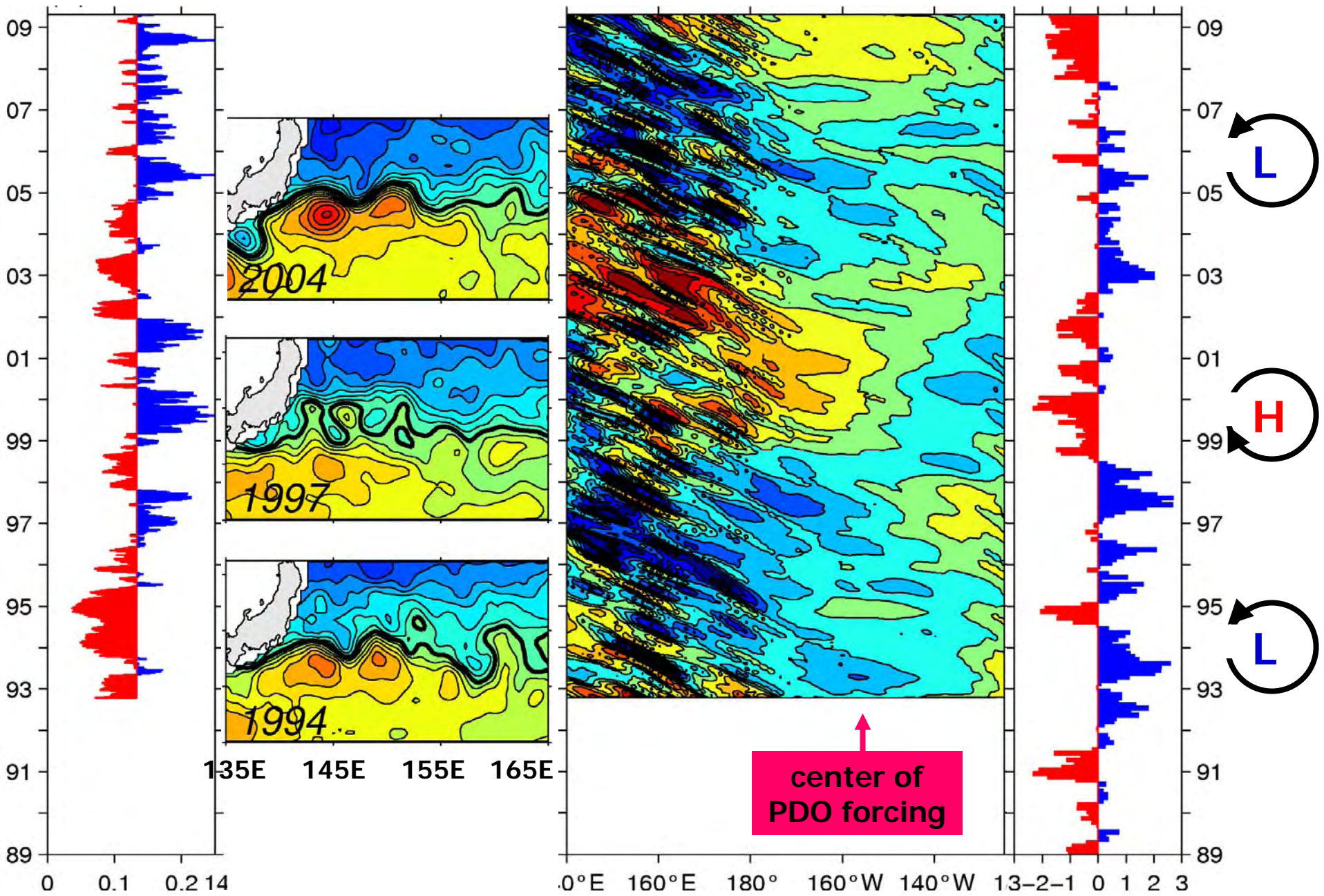
(e.g. Miller et al. 1998; Seager et al. 2001; Schneider et al. 2002; Qiu 2002; Taguchi et al. 2007; Ceballos et al. 2009)

EKE level

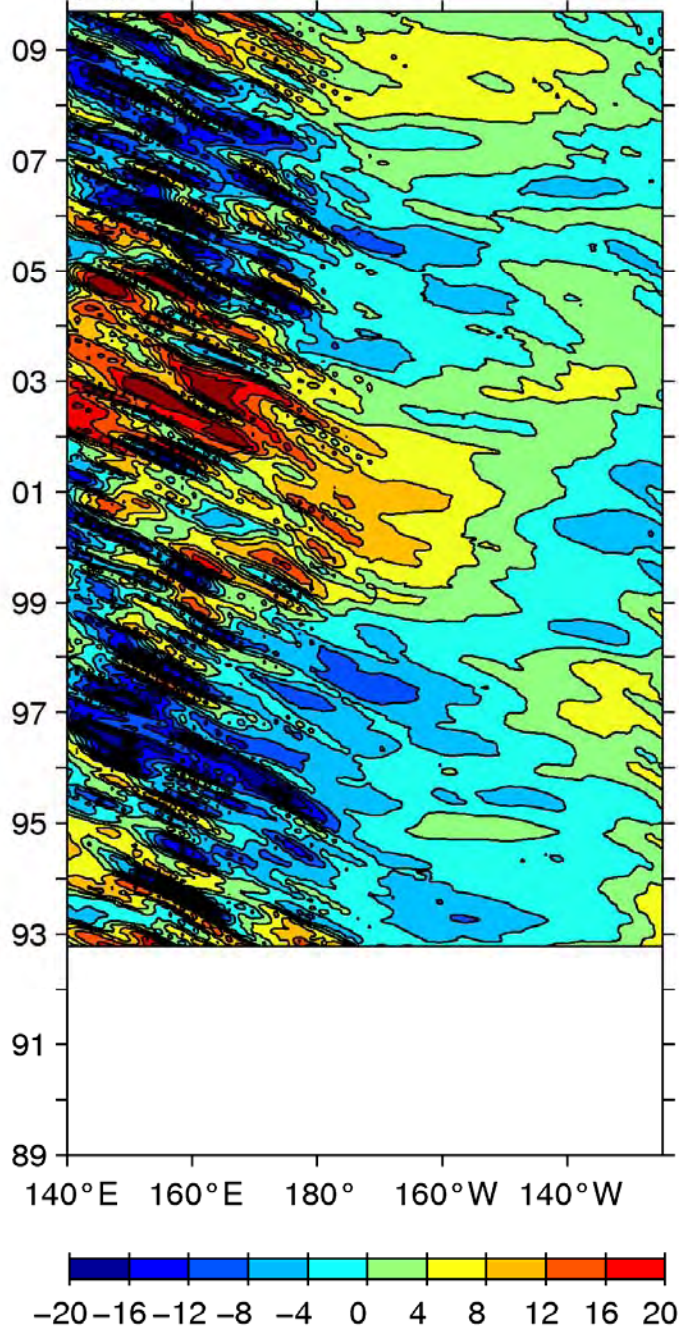
SSH field

SSHA along 34°N

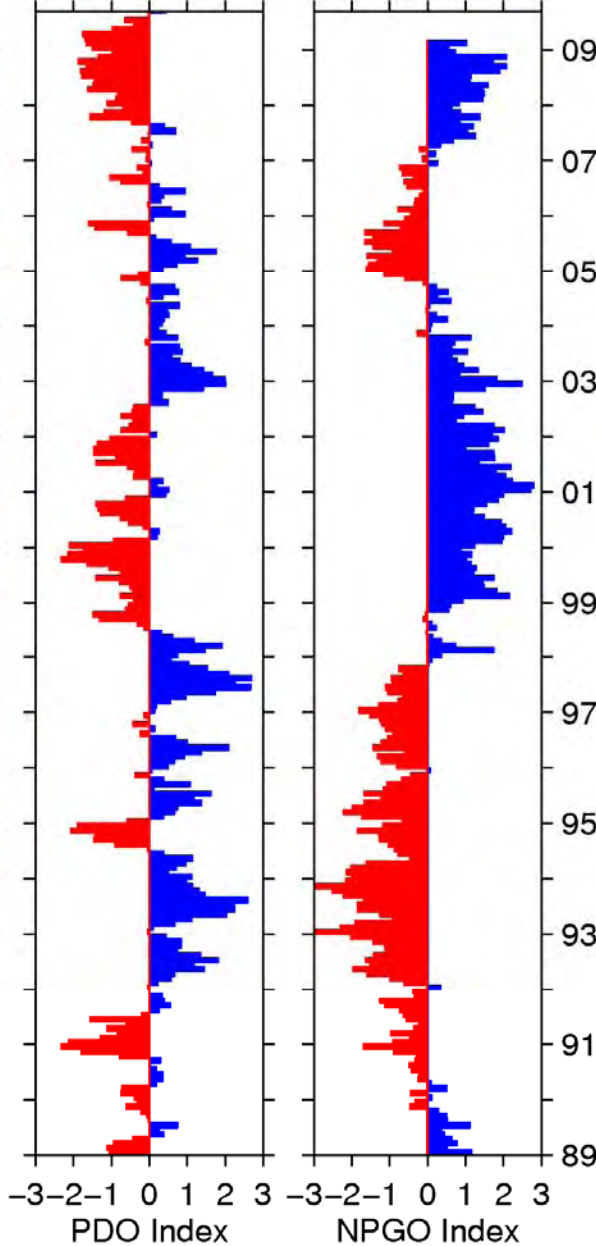
PDO index



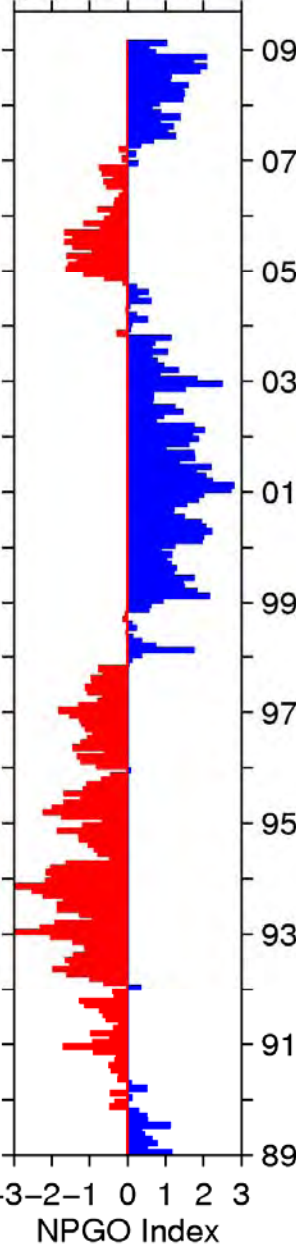
(a) SSHA



(b) PDO



(c) NPGO



(Di Lorenzo et al. 2008)

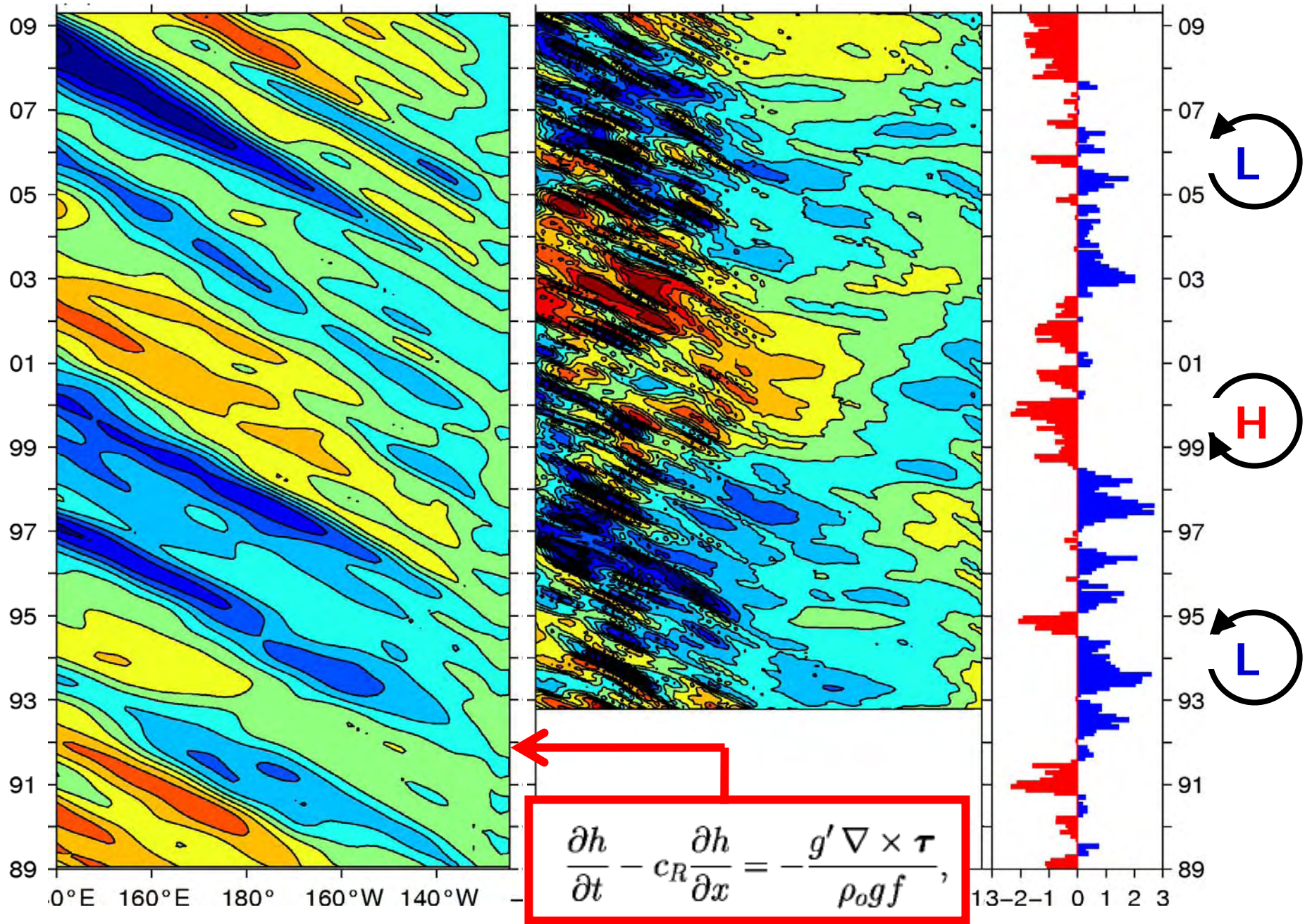
PDO-NPGO linear correlation:
-0.38 (monthly)
-0.62 (interannual)

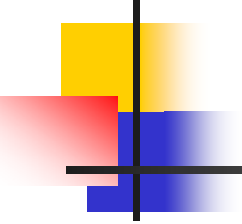
SSH Anomaly [cm]

Wind-forced SSHA along 34°N

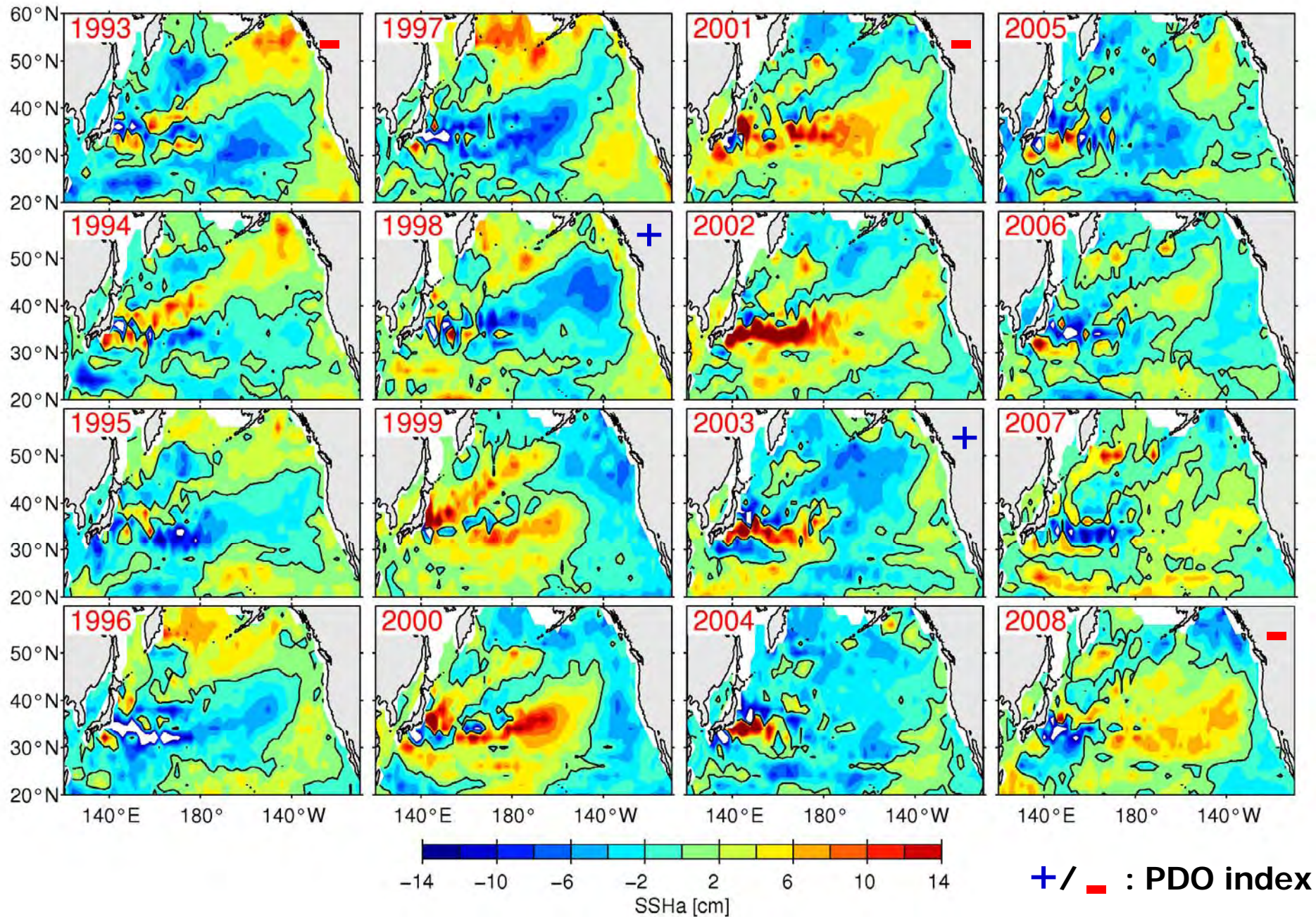
SSHA along 34°N

PDO index

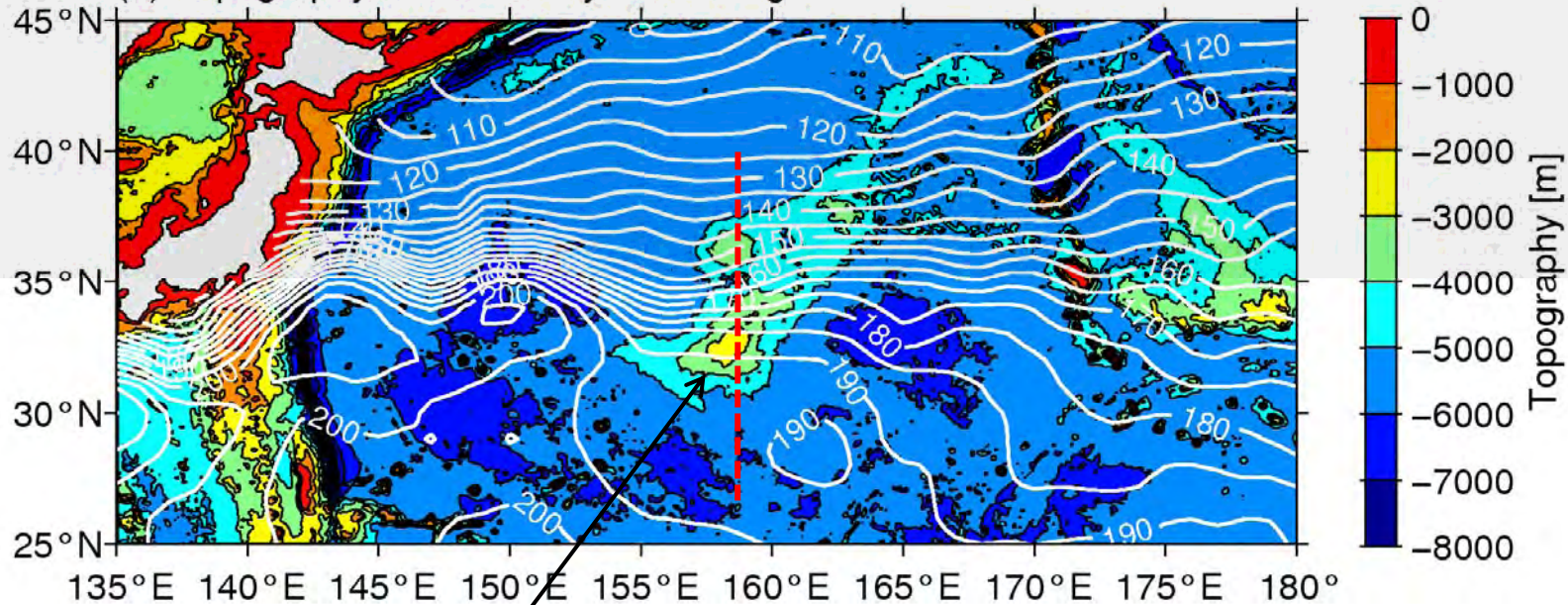


- 
-
- Q1: What causes the transitions between the stable and unstable dynamic states of the KE system?
 - Q2: What roles does the nonlinear ocean dynamics play?

Yearly SSH anomaly field in the North Pacific Ocean

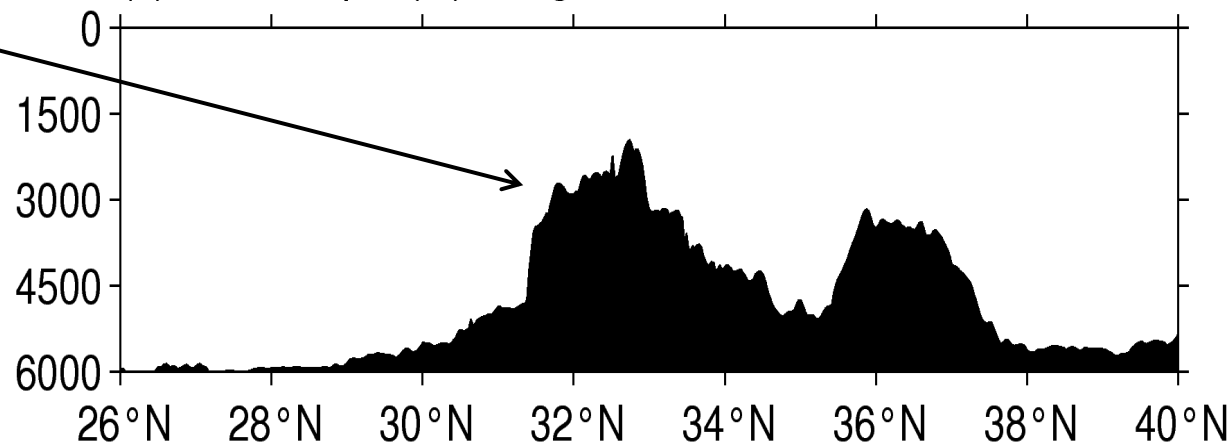


(a) Topography and Mean Dynamic Height

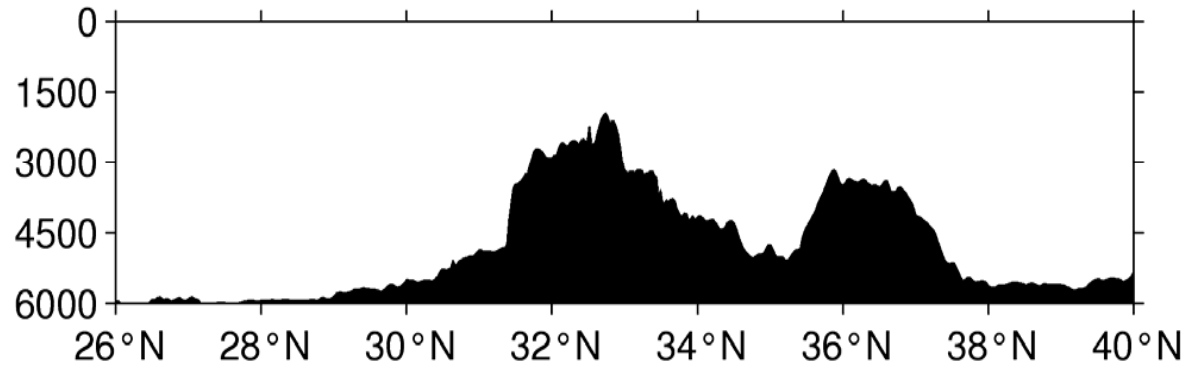


**Shatsky
Rise**

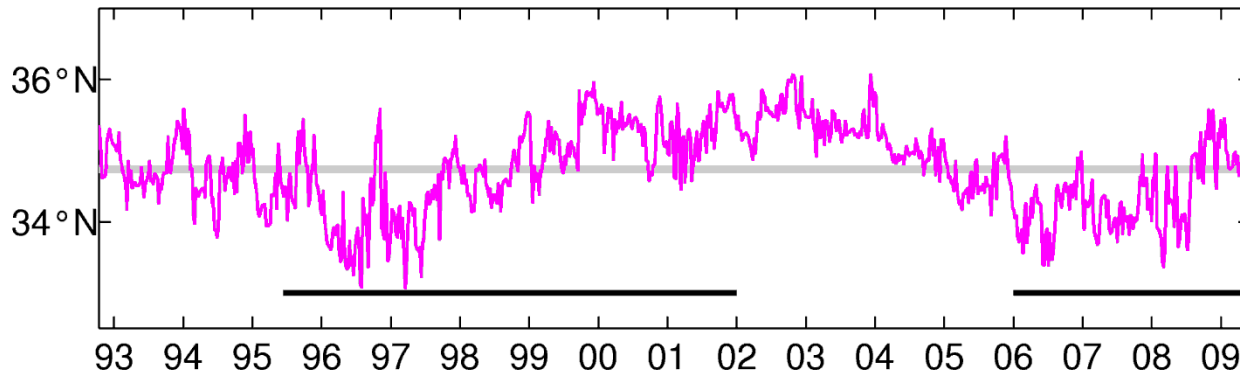
(b) Water Depth (m) along 158.2°E



(b) Water Depth (m) along 158.2°E

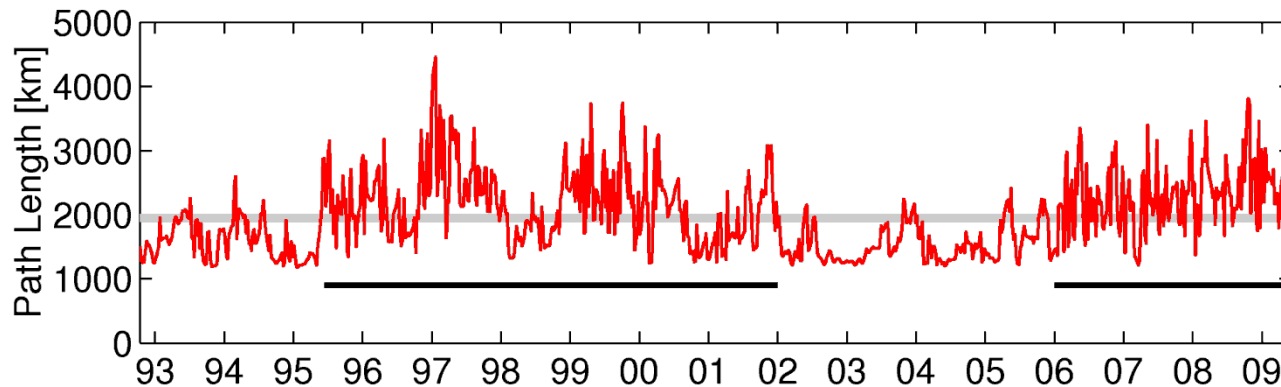


(c) Upstream KE Position (141°–165°E)



KE y-position

(a) Upstream KE Path Length (141°–153°E)



KE path length

Feedback of eddies to the modulating time-mean flow:

- Surface ocean vorticity equation:

$$\frac{g}{f} \frac{\partial(\nabla^2 \bar{h})}{\partial t} + \frac{g}{f} J(\bar{f} + \zeta, \bar{h}) = -\nabla \cdot (\overline{\mathbf{u}'\zeta'})$$

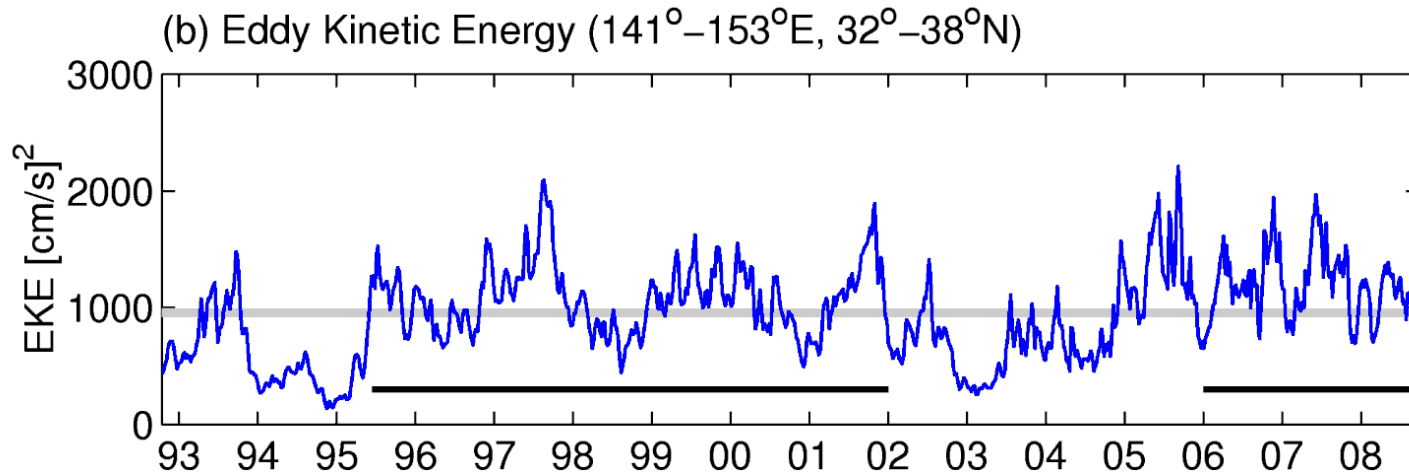
eddy-driven mean flow modulation

- Evaluate:

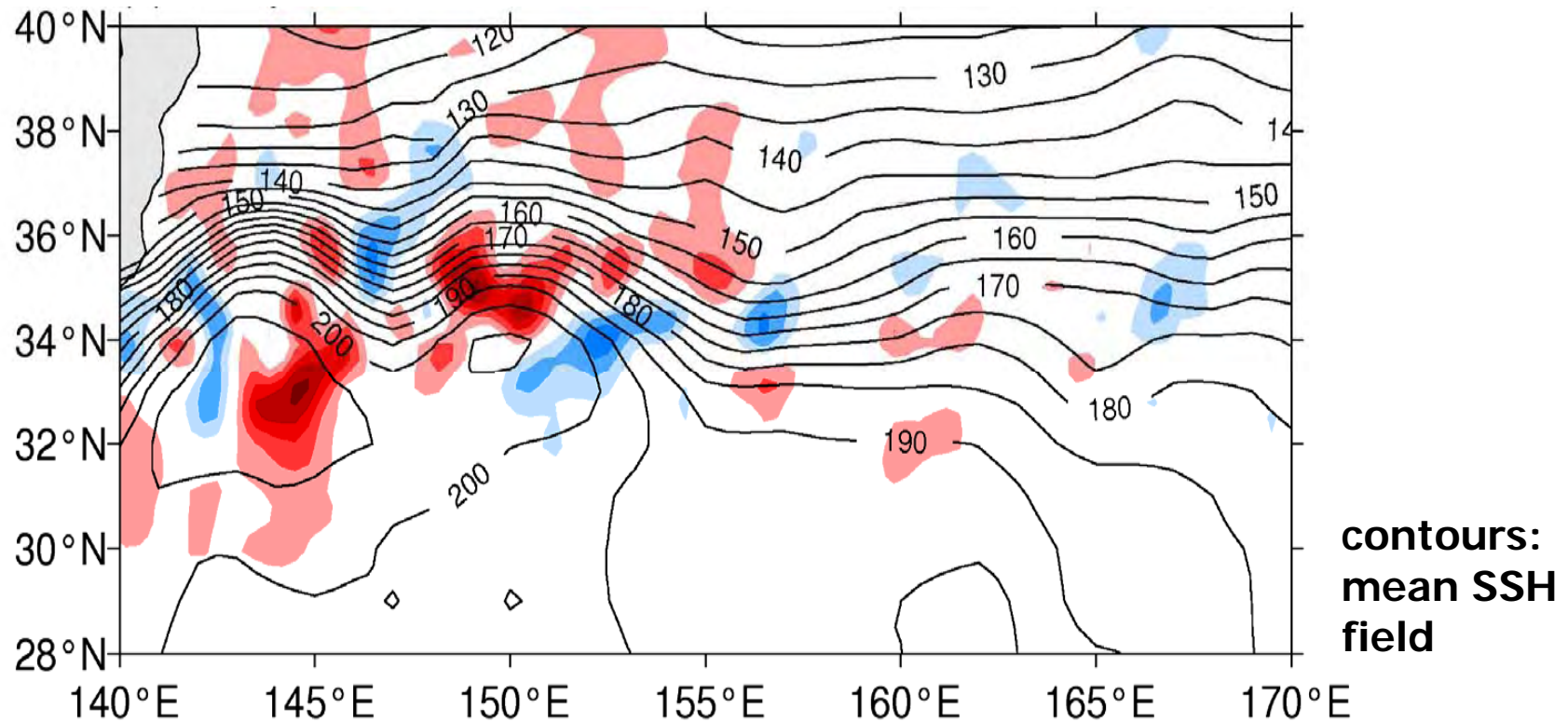
$$S(x, y, T) \equiv \frac{g}{f} \bar{h} = \nabla^{-2} [-\nabla \cdot (\overline{\mathbf{u}'\zeta'})]$$

mechanical feedback of eddies onto the time-varying SSH field (e.g. Hoskins et al. 1983, JAS)

- Regress $S(x, y, T)$ field to the observed EKE time series:

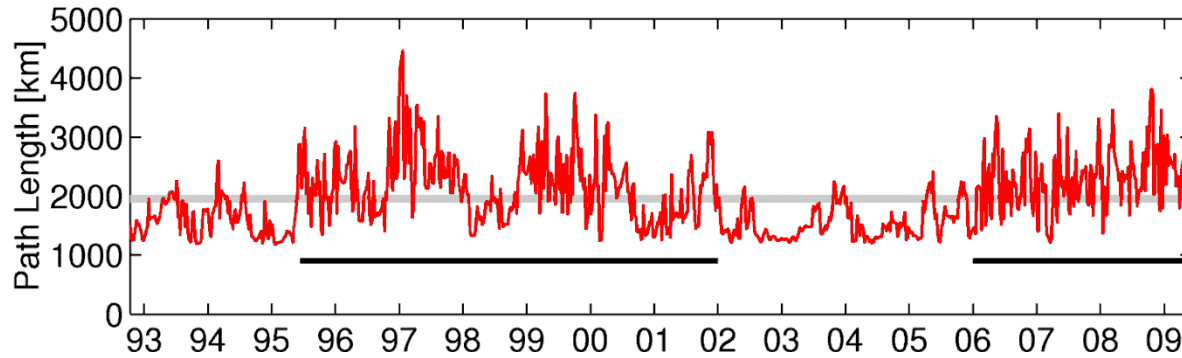


Eddy-forced $S(x,y,T)$ field regressed to the EKE time series



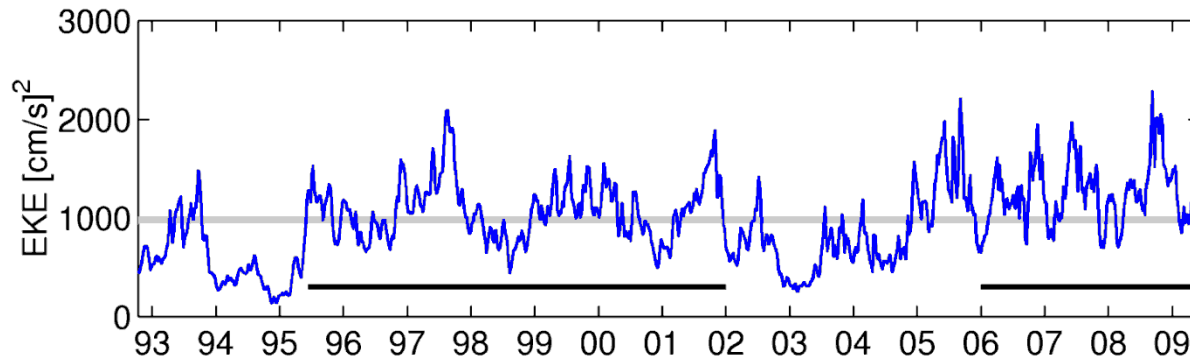
- **+**: anticyclonic forcing vs . **-**: cyclonic forcing
- In the upstream KE region, enhanced eddy variability works to increase the intensity of the southern RG.
- Enhanced eddy variability strengthens the two quasi-stationary meanders (cf. Rossby lee-wave dynamics)

(a) Upstream KE Path Length (141°–153°E)



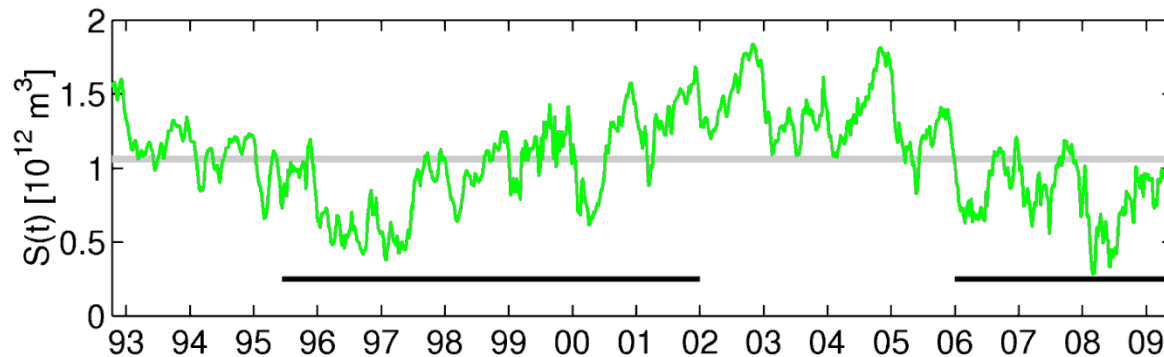
KE path length

(b) Eddy Kinetic Energy (141°–153°E, 32°–38°N)



Level of EKE

(d) KE Recirculation Gyre Strength

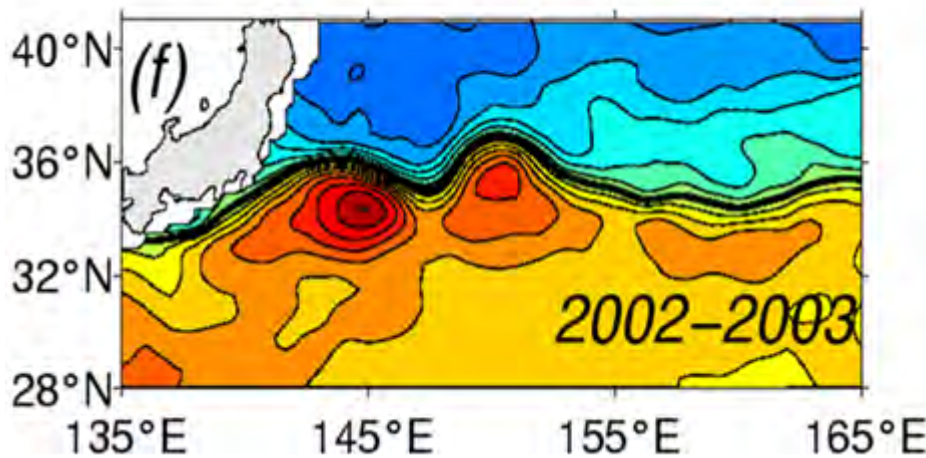


RG strength

Stable yrs: 1993-94, 2002-04

Unstable yrs: 1996-2001, 2006-08

Strong Jet/RG-Low EKE State



+ PDO

• Bypassing S.R. and reduced EKE level

• Strengthening RG and northerly KE jet

• Incoming positive SSHA

• Ekman convergence in the east

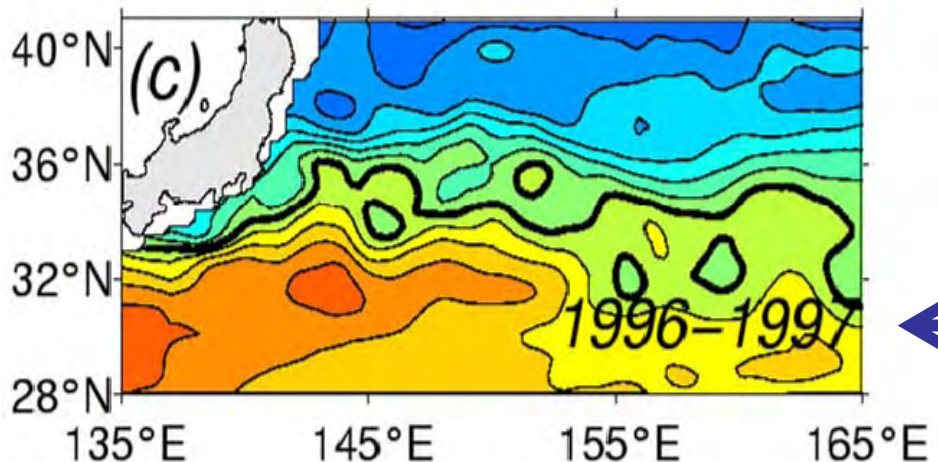
• Ekman divergence in the east

• Incoming negative SSHA

• Weakening RG and southerly KE jet

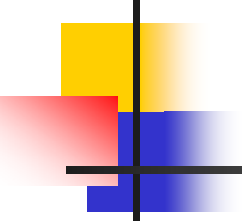
• Overriding S.R. and enhancing local EKE level

Weak Jet/RG-High EKE State

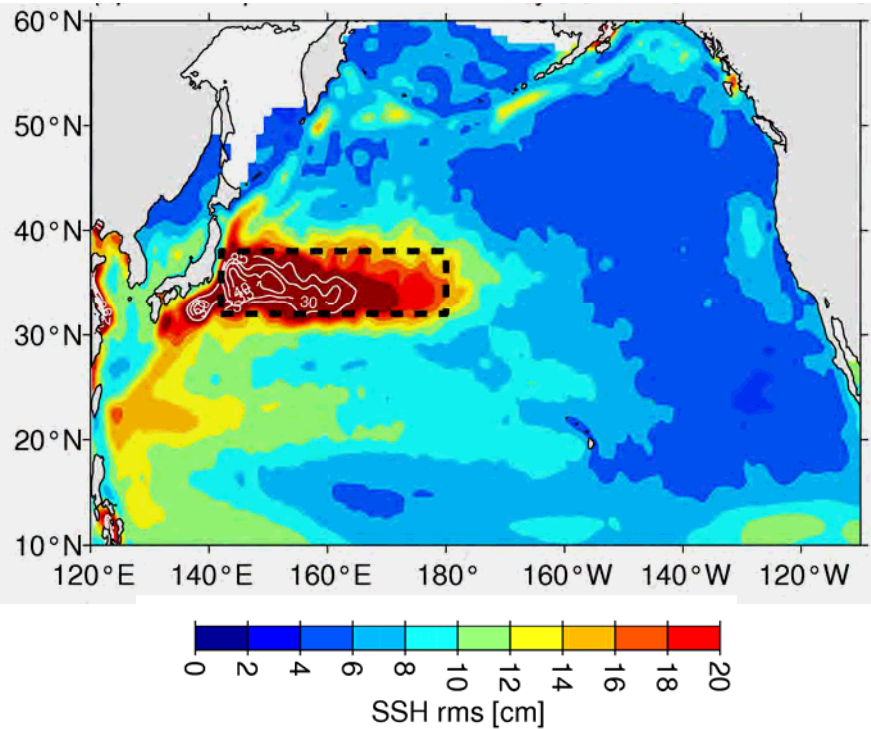


- PDO

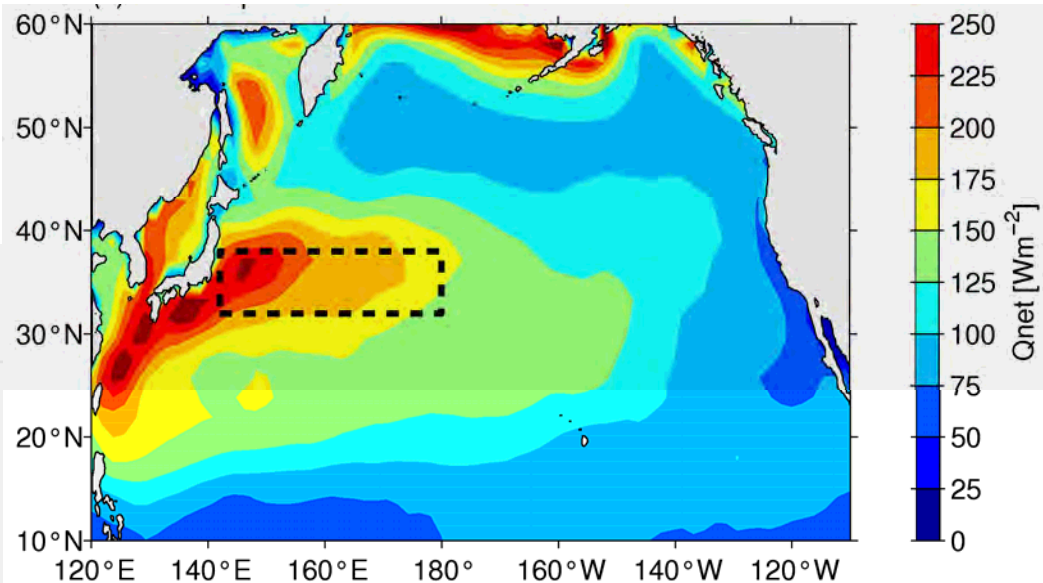
- PDO

- 
-
- Q1: What causes the transitions between the stable and unstable dynamic states of the KE system?
 - Q2: What roles does the nonlinear ocean dynamics play?
 - **Q3: What determines the observed, preferred decadal timescale?**

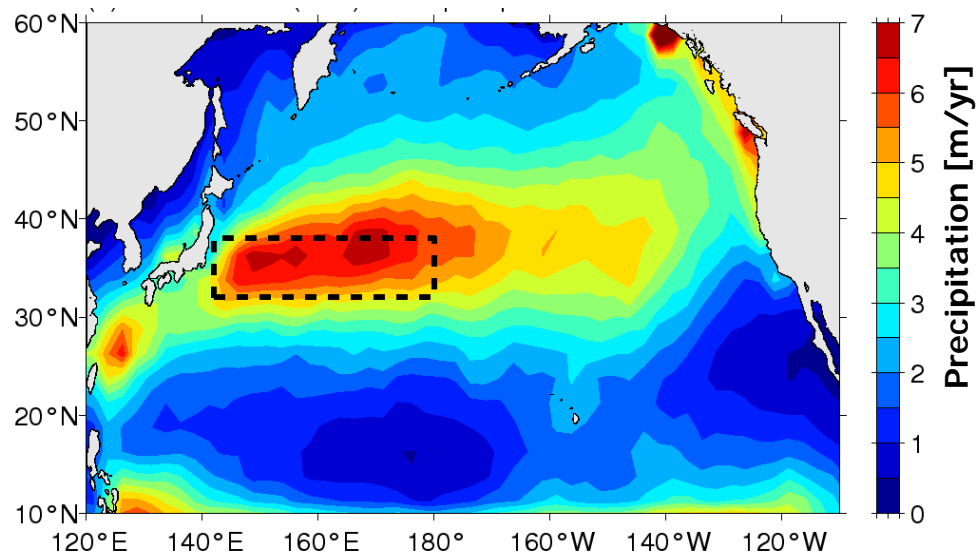
RMS SSH variability (AVISO data)



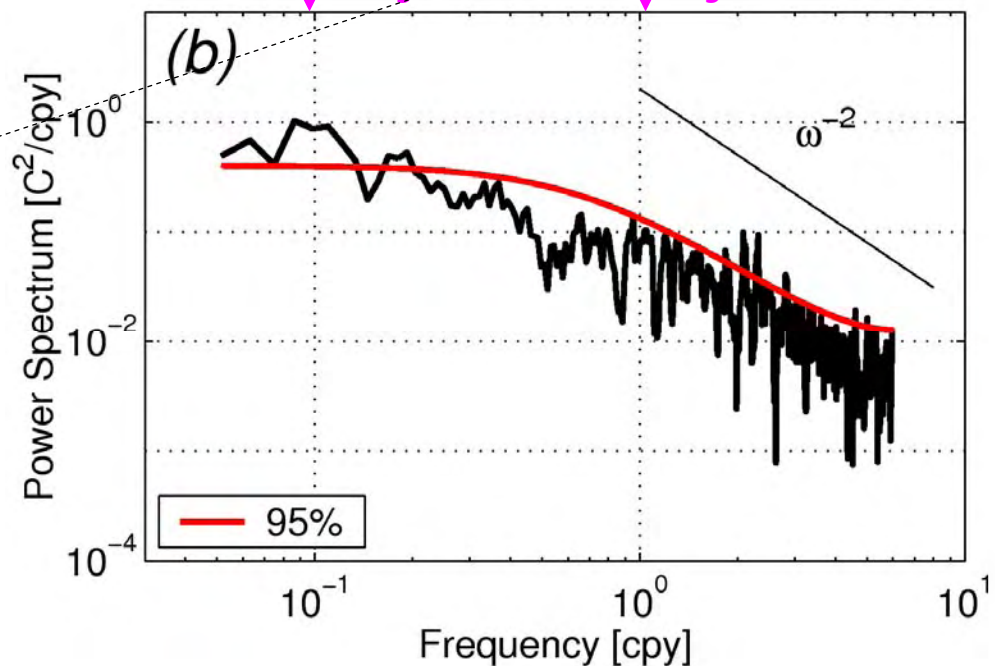
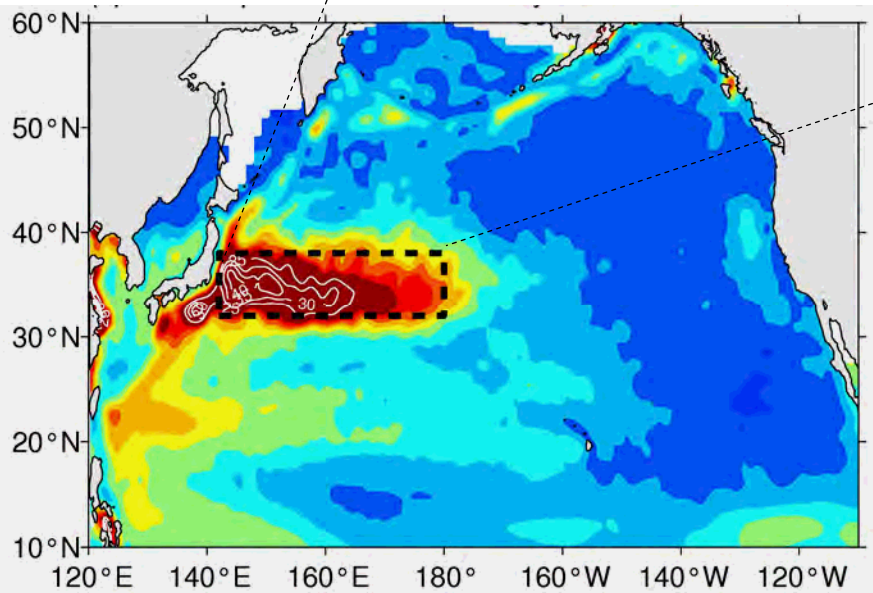
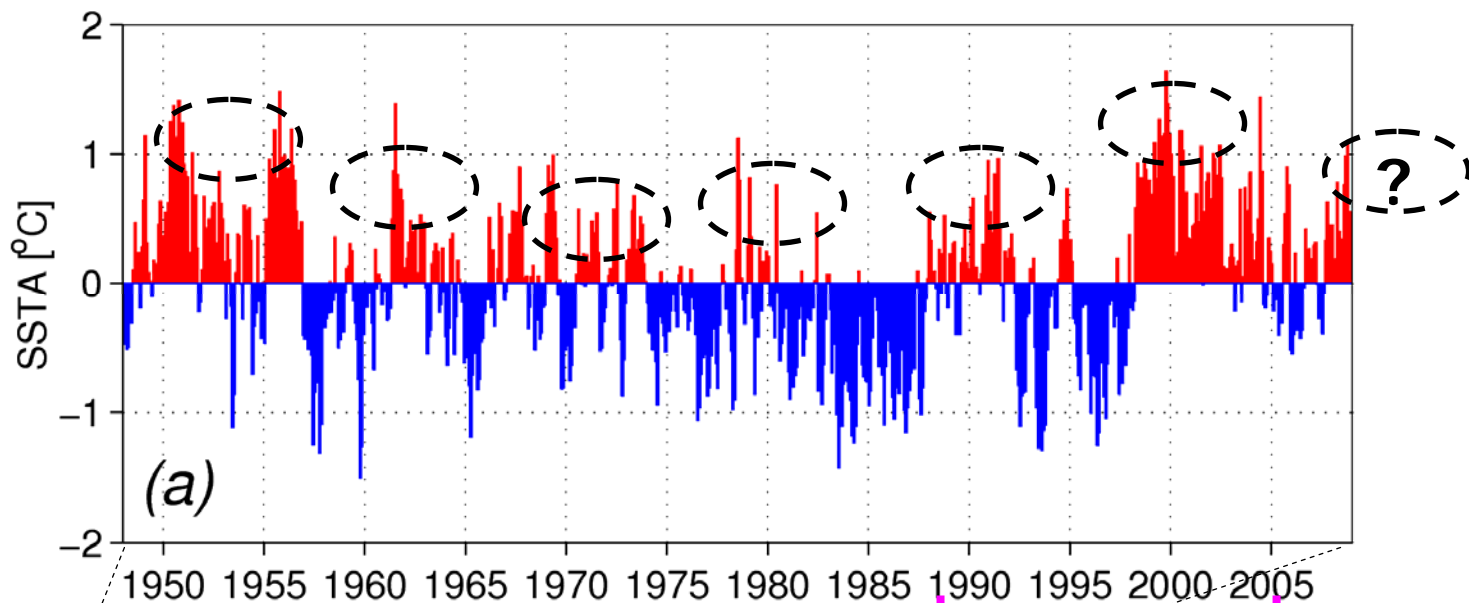
JFM rms net surface heat flux variability (NCEP reanalysis)



JFM precipitation (proxy for winter stormtracks)



SST anomaly time series in the KE region



An idealized air-sea coupled system:

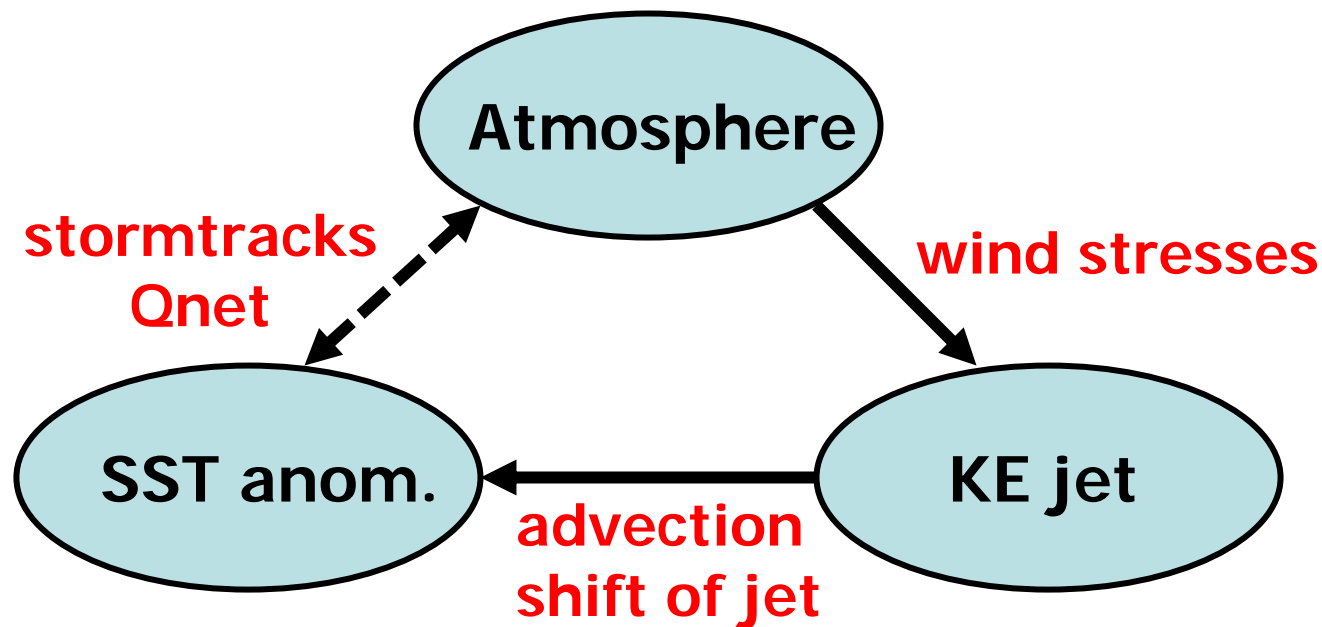
$$\frac{\partial h(x,t)}{\partial t} - c_R \frac{\partial h(x,t)}{\partial x} = -\frac{g' \text{curl} \boldsymbol{\tau}}{\rho_o g f} \quad (1)$$

$$\frac{\partial T(t)}{\partial t} = a \overline{h(t)} - \lambda T(t) + q(t) \quad (2)$$

$$-\frac{g' \text{curl} \boldsymbol{\tau}}{\rho_o g f} = \sum_{n=1}^2 \sin\left(\frac{n\pi x}{W}\right) w_n(t) + b \sin\left(\frac{2\pi x}{W}\right) T(t) \quad (3)$$

intrinsic

feedback



SST's impact from the lagged correlation approach

(Czaja and Frankignoul 1999, 2002)

Let an atmospheric variable $C(t)$ be:

$$C(t) = f(t) + F(T) \\ \sim f(t) + b T(t)$$

where f represents intrinsic atmospheric processes, b , the dynamic feedback coefficient, and T , SST anomalies.

Taking lagged correlation with $T(t-m)$ and ensemble average:

$$\{T(t-m)C(t)\} = \{T(t-m)f(t)\} + b\{T(t-m)T(t)\}$$

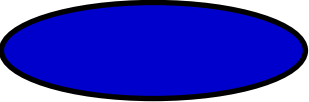

if $m >$ a few weeks

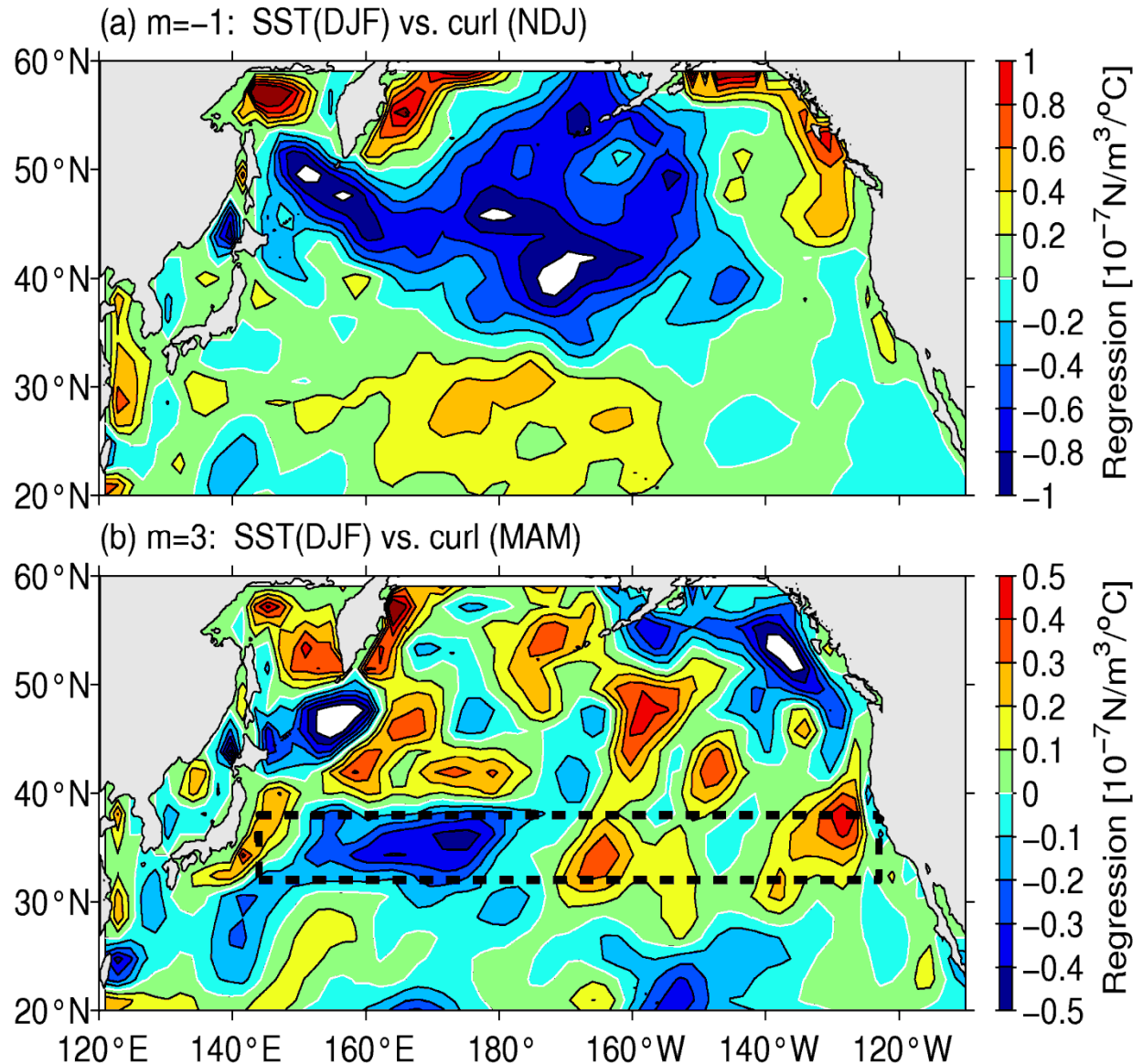
The covariance between SST and $C(t)$ when SST leads is proportional to the strength of the feedback.

(cf. Liu and Wu 2004; Frankignoul and Sennechael 2007)

Lagged regression between KE SSTA and NP curl-tau field

- NCEP reanalysis data (1950-2008)
- ENSO signals (Nino 3.4) regressed out
- Different curl patterns with +/- lag

- 
 $p' > 0$; curl-tau < 0
- 
 $p' < 0$; curl-tau > 0



Parameter values appropriate for N. Pacific:

$$y = 35^\circ\text{N}, \quad c_R = 0.033 \text{ m/s}$$

band of action

$$W = 95^\circ\text{lon.}, \quad L = 40^\circ\text{lon.}$$

band configuration

→ $a = 2.73 \times 10^{-7} \text{ K/m/s}$

advection parameter
(likely underestimated!)

$$\lambda = 1/129.2 \text{ days}$$

oceanic damping timescale

$$|\widehat{w}_1(\omega)|^2 = 1.127 \times 10^{-18} \text{ m}^2/\text{s}^2/\text{cpy}$$

power of stochastic wind stress forcing (n=1)

$$|\widehat{w}_2(\omega)|^2 = 0.643 \times 10^{-18} \text{ m}^2/\text{s}^2/\text{cpy}$$

power of stochastic wind stress forcing (n=2)

$$|\widehat{q}(\omega)|^2 = 2.89 \times 10^{-15} \text{ K}^2/\text{s}^2/\text{cpy}$$

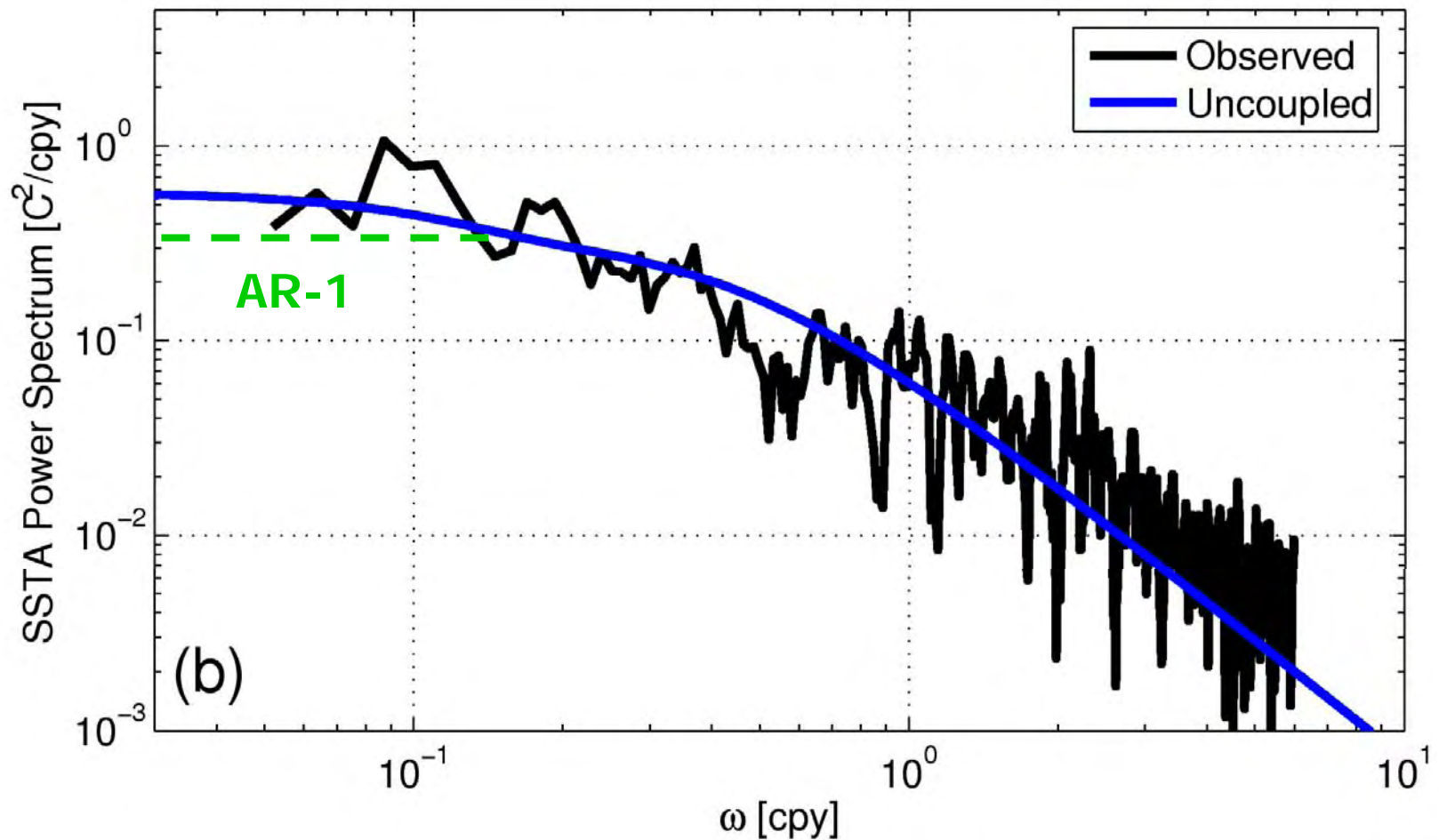
power of stochastic heat flux forcing

→ $b = 6.64 \times 10^{-10} \text{ m/s/K}$

air-sea coupling parameter

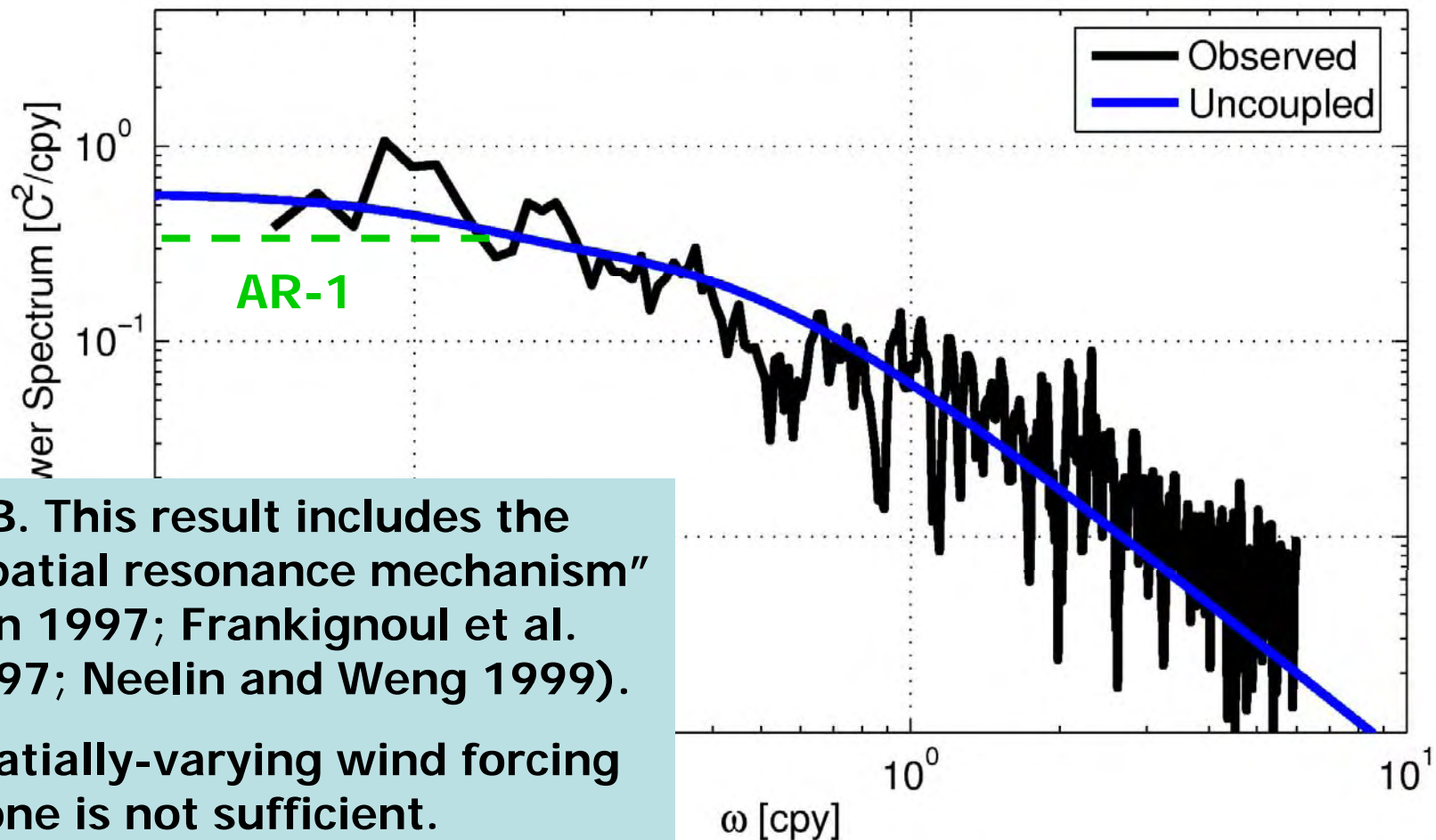
Uncoupled case (b=0)

$$|\widehat{T}(\omega)|_{\text{uncoupled}}^2 = \frac{1}{\lambda^2 + \omega^2} \left[a^2 \sum_{n=1}^2 |P_n(\omega)|^2 |\widehat{w}_n(\omega)|^2 + |\widehat{q}(\omega)|^2 \right]$$



Uncoupled case (b=0)

$$|\widehat{T}(\omega)|_{\text{uncoupled}}^2 = \frac{1}{\lambda^2 + \omega^2} \left[a^2 \sum_{n=1}^2 |P_n(\omega)|^2 |\widehat{w}_n(\omega)|^2 + |\widehat{q}(\omega)|^2 \right]$$

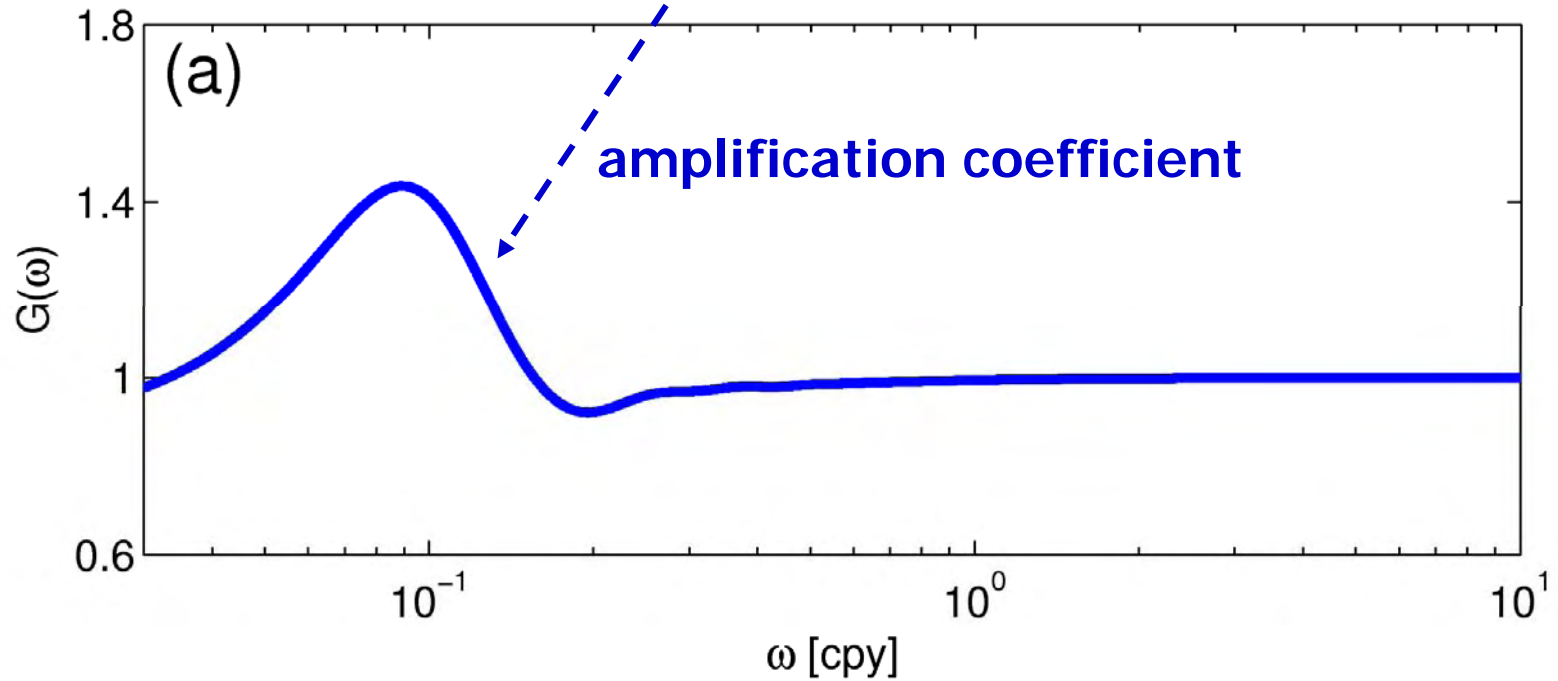


N.B. This result includes the “spatial resonance mechanism” (Jin 1997; Frankignoul et al. 1997; Neelin and Weng 1999).

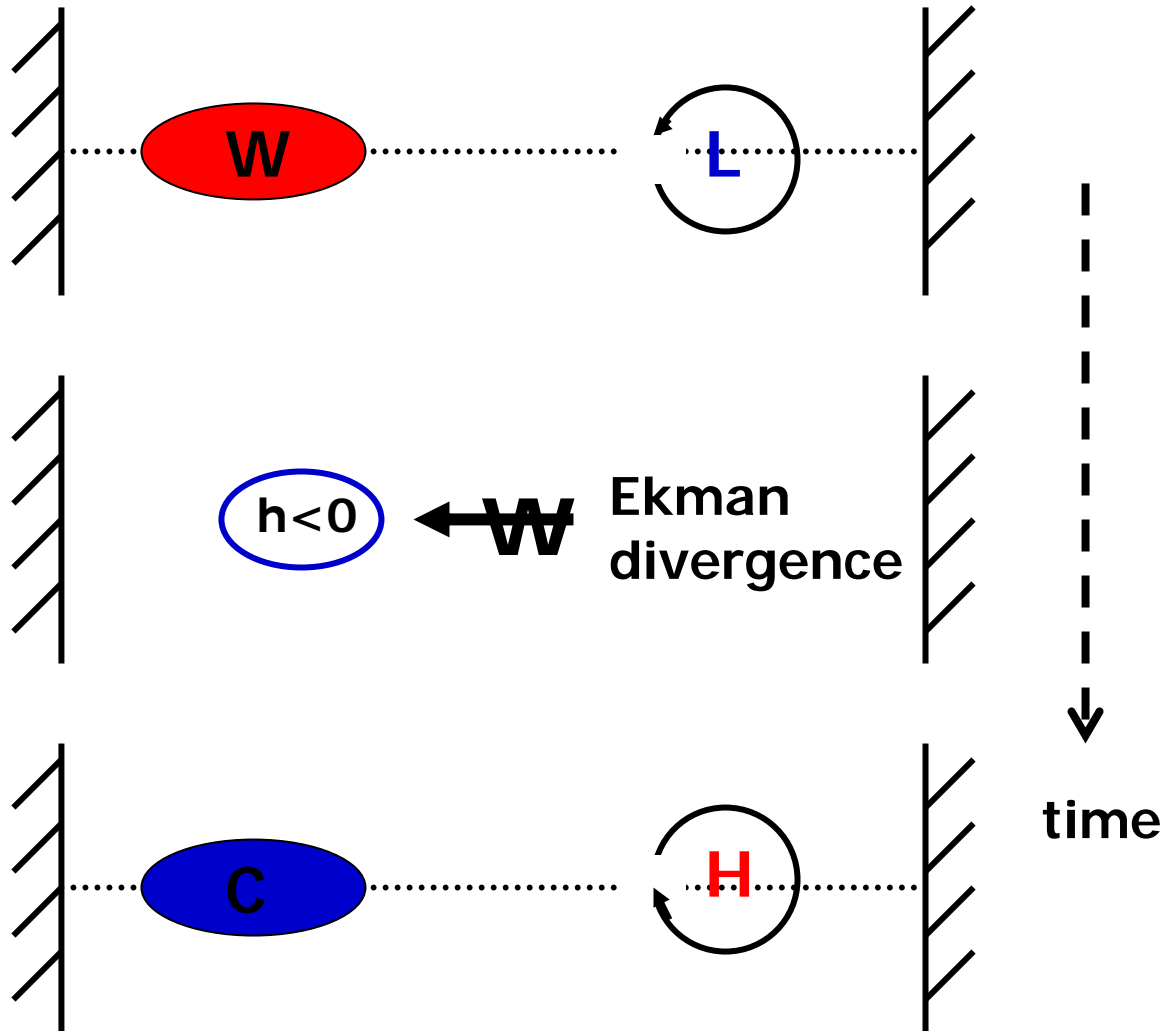
Spatially-varying wind forcing alone is not sufficient.

Coupled case ($b \neq 0$)

$$|\widehat{T}(\omega)|_{\text{coupled}}^2 = \left| \frac{\lambda + i\omega}{\lambda + i\omega - abP_2(\omega)} \right|^2 |\widehat{T}(\omega)|_{\text{uncoupled}}^2$$



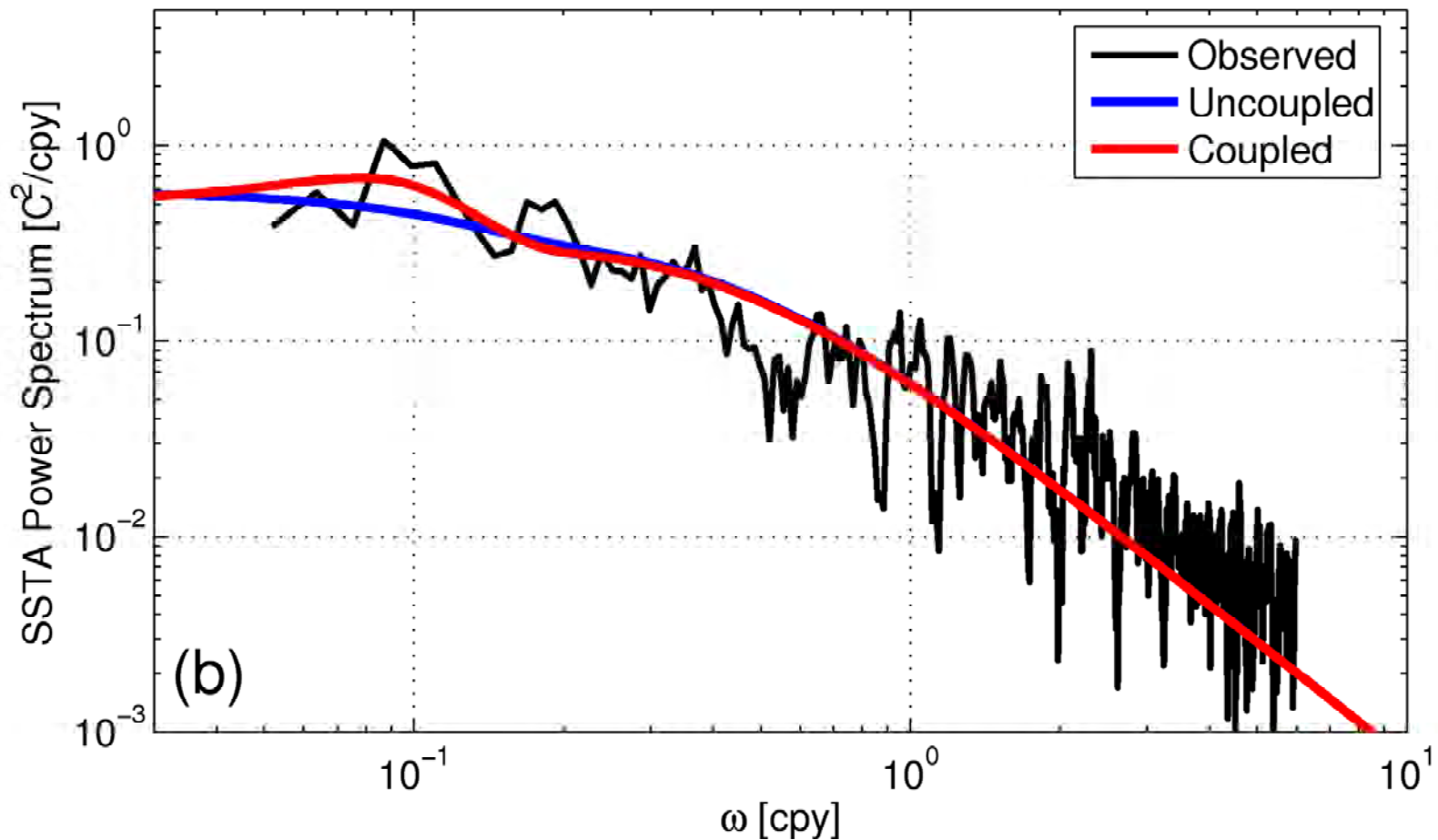
Schematic for the coupled oscillation



half of the optimal period $\sim (W/2)/c_R$

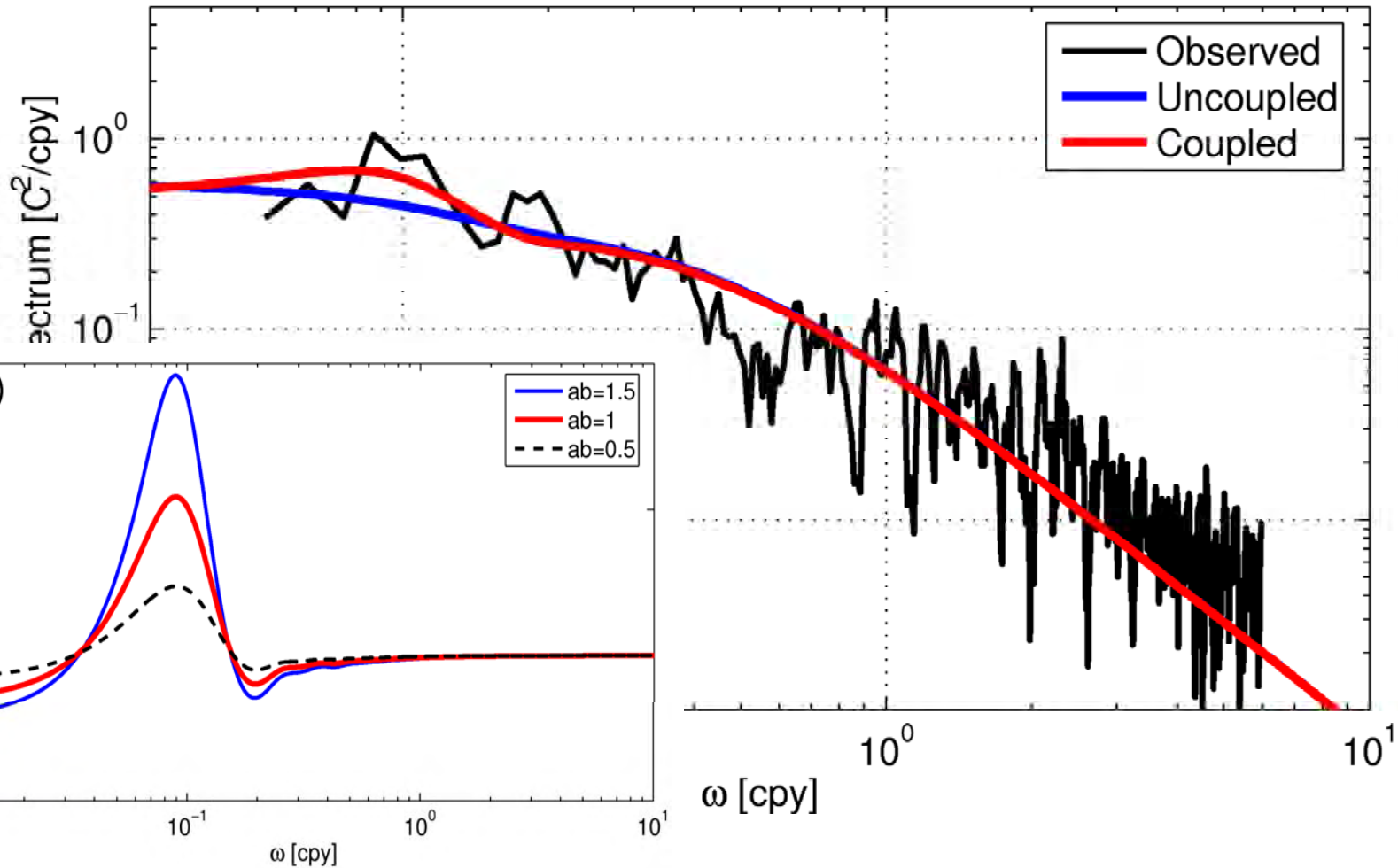
Coupled case ($b \neq 0$)

$$|\widehat{T}(\omega)|_{\text{coupled}}^2 = \left| \frac{\lambda + i\omega}{\lambda + i\omega - abP_2(\omega)} \right|^2 |\widehat{T}(\omega)|_{\text{uncoupled}}^2$$



Coupled case ($b \neq 0$)

$$|\widehat{T}(\omega)|_{\text{coupled}}^2 = \left| \frac{\lambda + i\omega}{\lambda + i\omega - abP_2(\omega)} \right|^2 |\widehat{T}(\omega)|_{\text{uncoupled}}^2$$



Summary

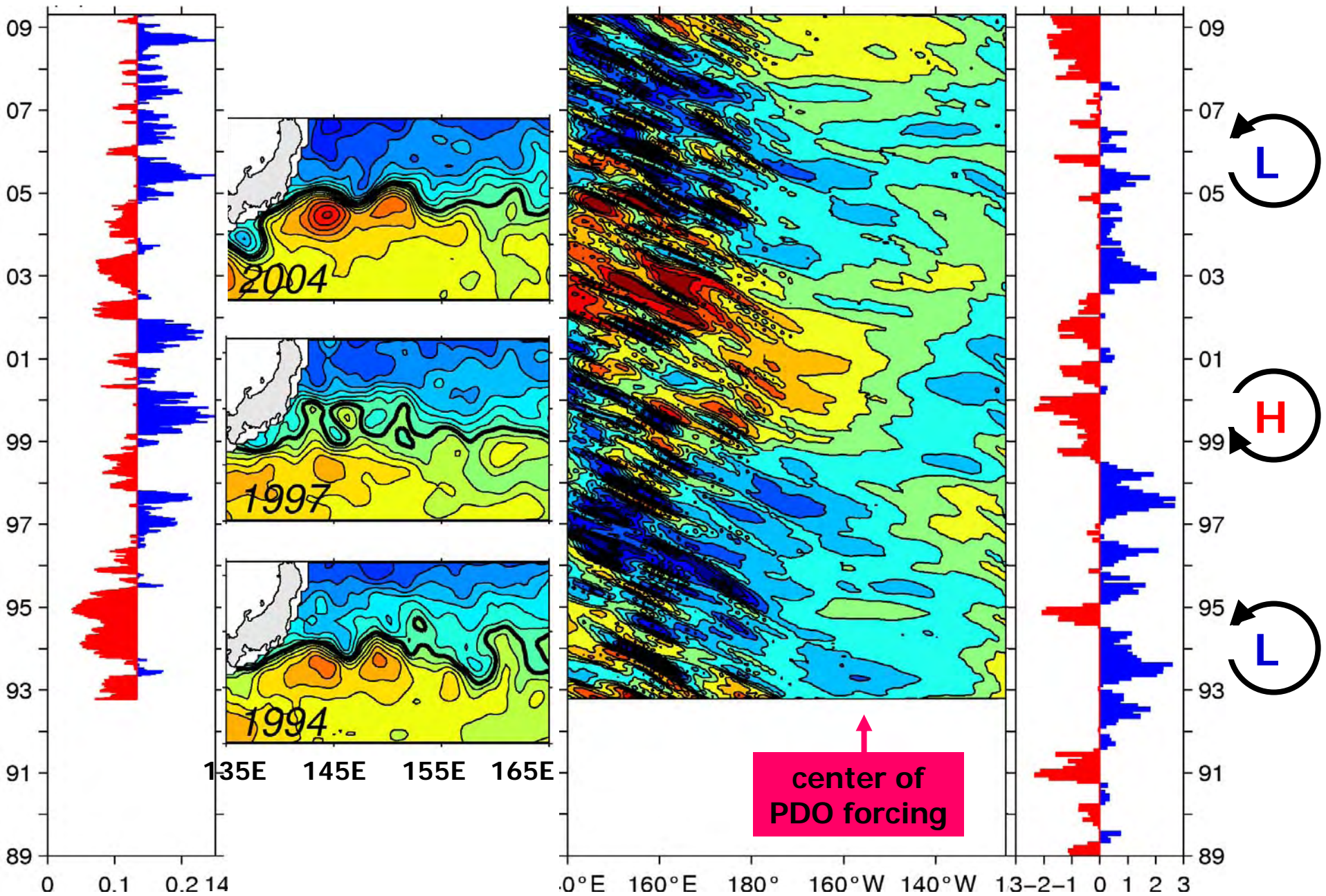
- Decadal variability dominates SSH, SST and other oceanic variables in the KE region. With the observed wind stress data, this variability can be predicted with a 3~4 yr lead.
- Ocean dynamics alone “reddens” the SST spectrum, but generates no decadal spectral peak as observed.
- Wintertime KE SST anomalies induce overlying-high and downstream-low pressure anomalies. This feedback favors a coupled mode with a ~10 yr timescale.
- Nonlinear eddy-mean flow interaction can increase the amplitude of this coupled mode by enhancing regional SST anomalies (via parameter a).
- While the variance explained by this coupled mode is small for atmosphere (~15%), it is the **driving force** for decadal changes in oceanic variables: KE’s path, SST, eddy level, and RG intensity.

EKE level

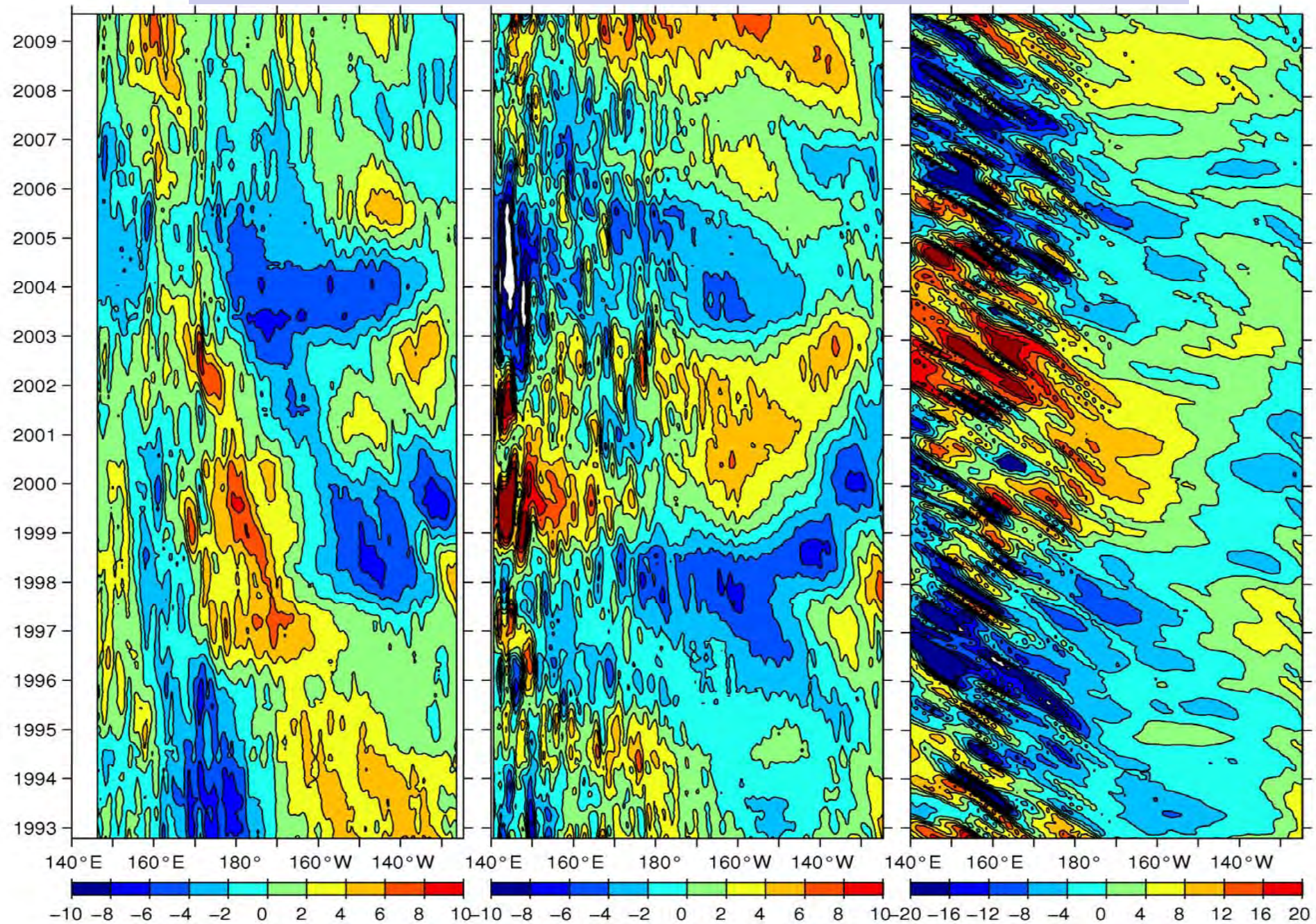
SSH field

SSHA along 34°N

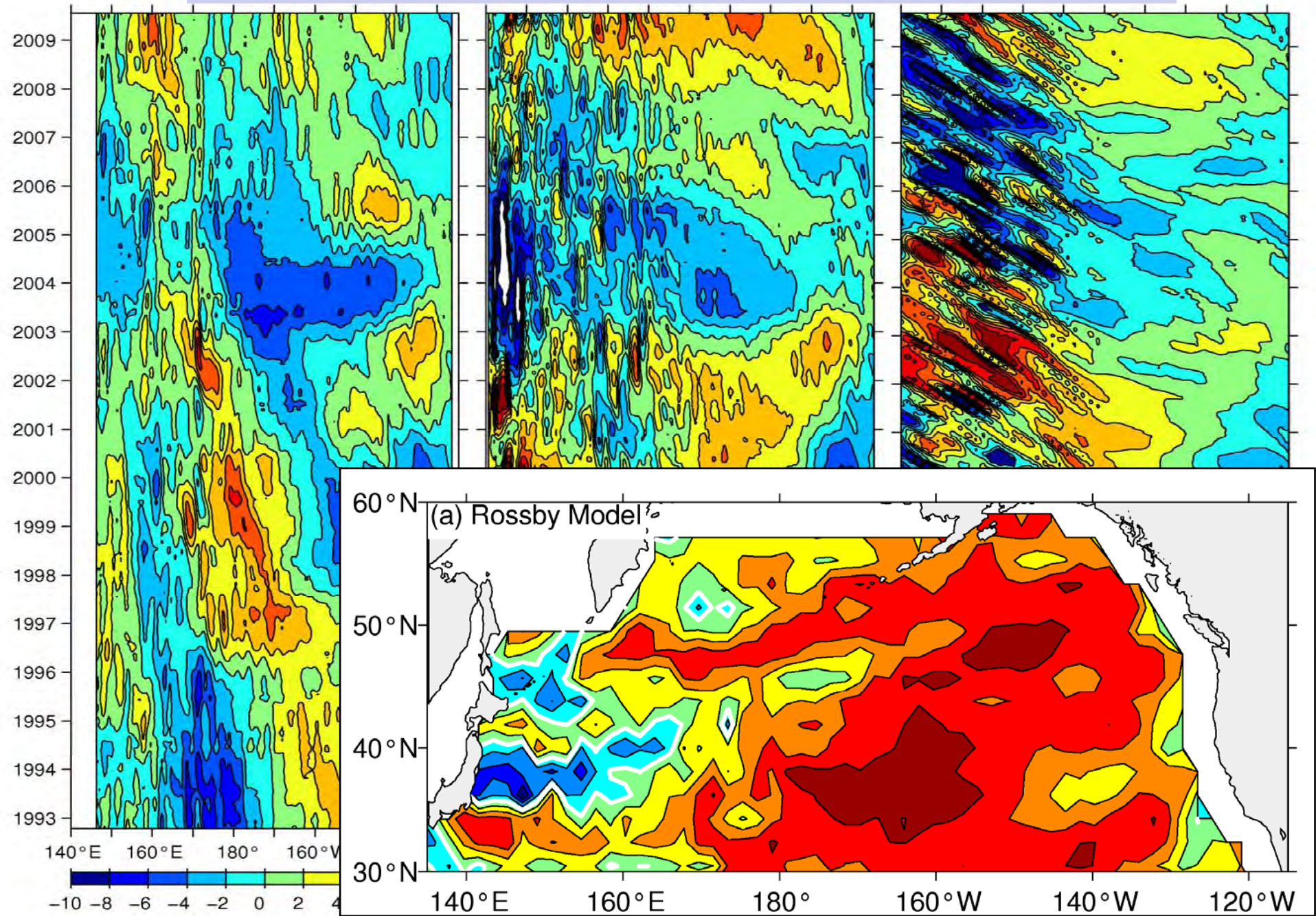
PDO index



Contrast 3 latitude bands: 45-50N, 37-42N, 32-34N

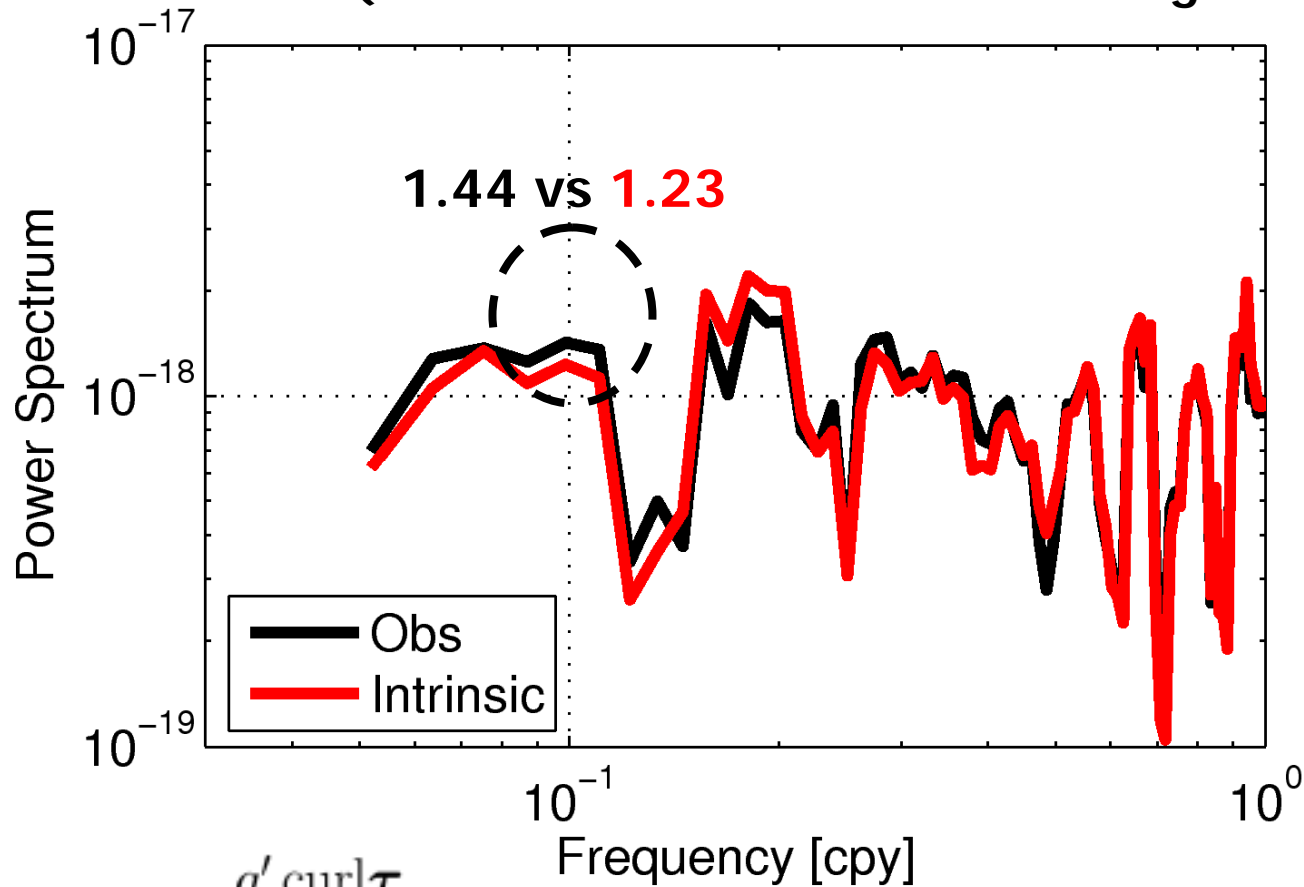


Contrast 3 latitude bands: 45-50N, 37-42N, 32-34N



How large is the SST-induced wind forcing?

(in the eastern half of the NP along the KE band)

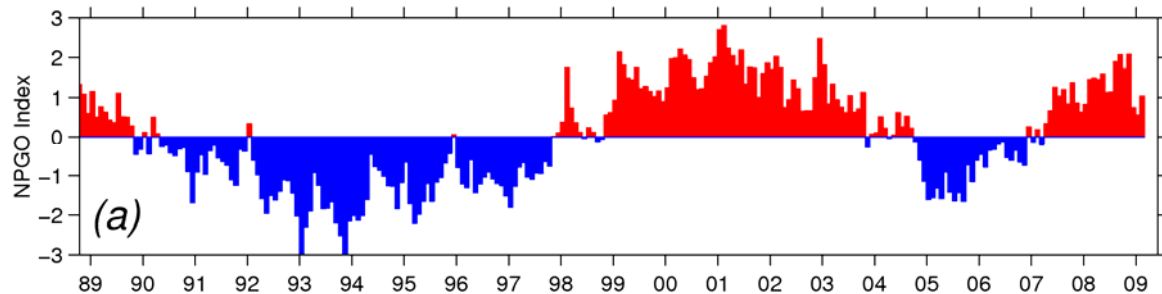


$$-\frac{g' \text{curl} \tau}{\rho_o g f}$$

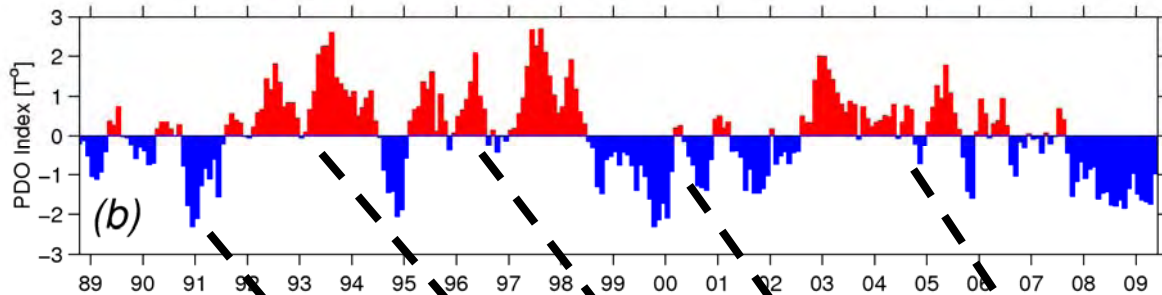


$$-\frac{g' \text{curl} \tau}{\rho_o g f} - b \sin \left(\frac{2\pi x}{W} \right) T(t)$$

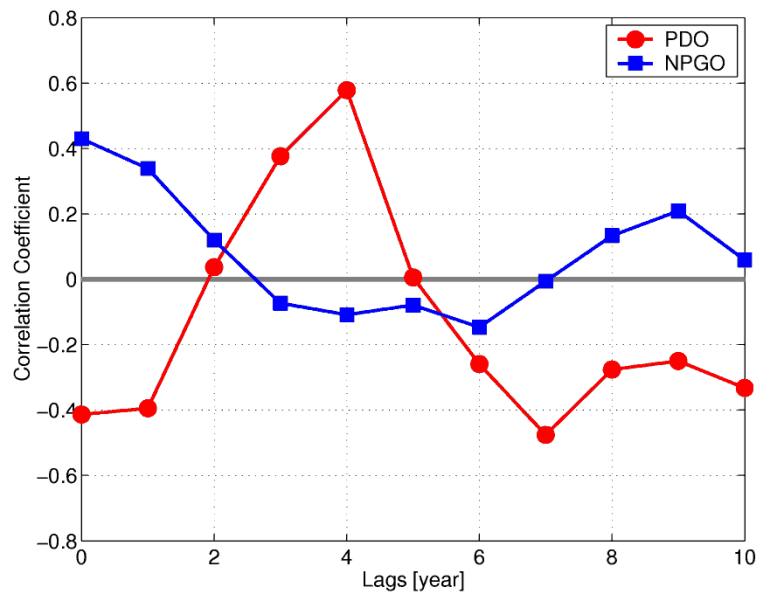
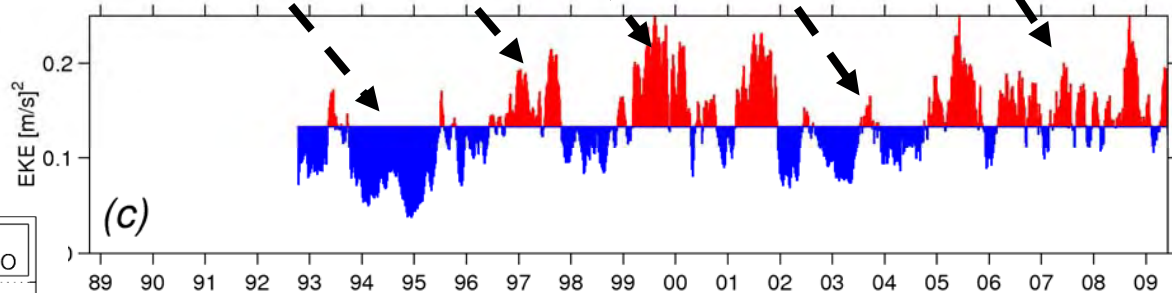
NPGO index



PDO index



EKE level



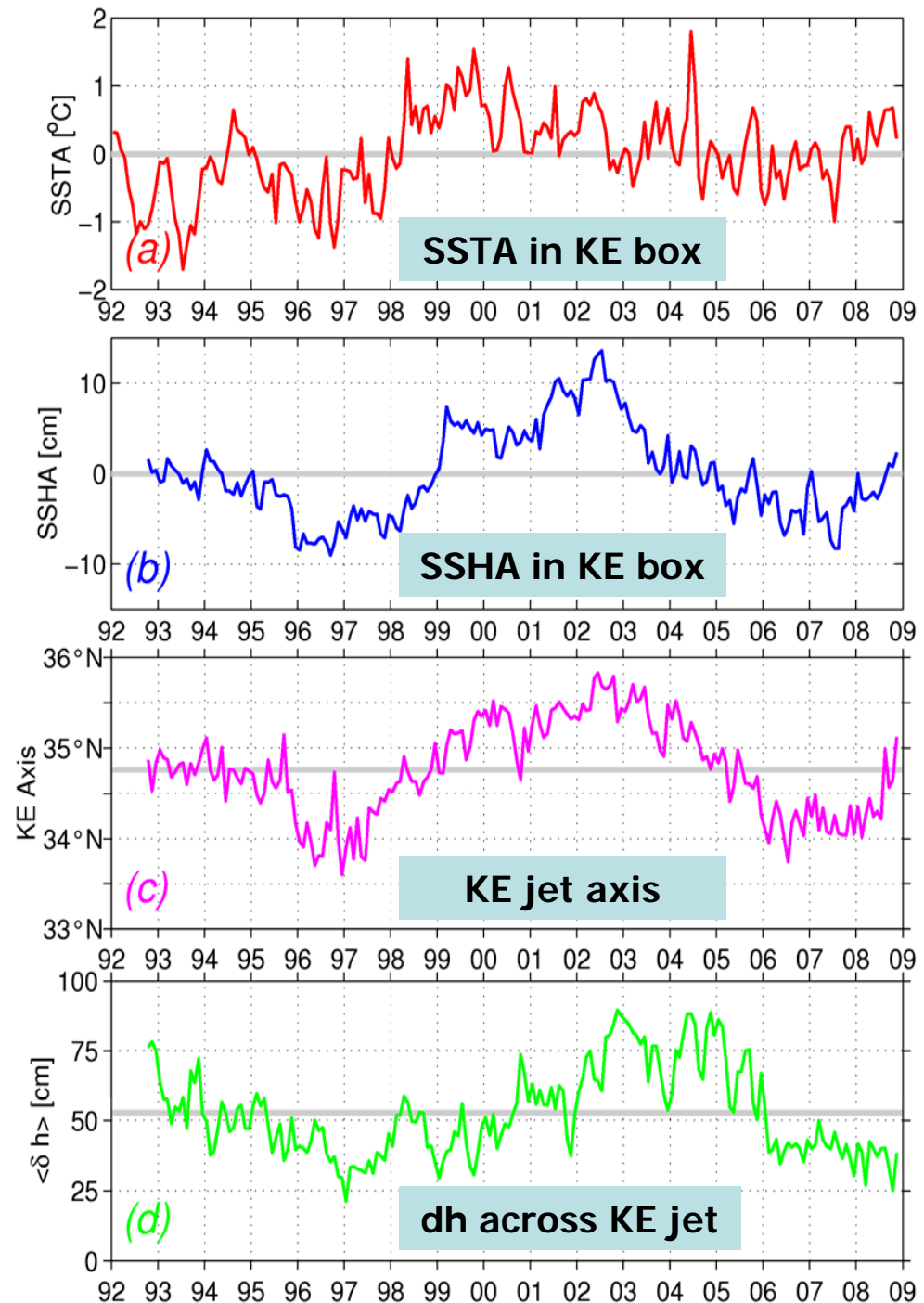
Extended Hasselmann model

$$\frac{\partial T(t)}{\partial t} = a \overline{h(t)} - \lambda T(t) + q(t)$$

where

$$\overline{h(t)} \equiv \frac{1}{L} \int_{-W}^{-W+L} h(x, t) dx$$

averaged SSHA in the KE box



An idealized air-sea coupled system:

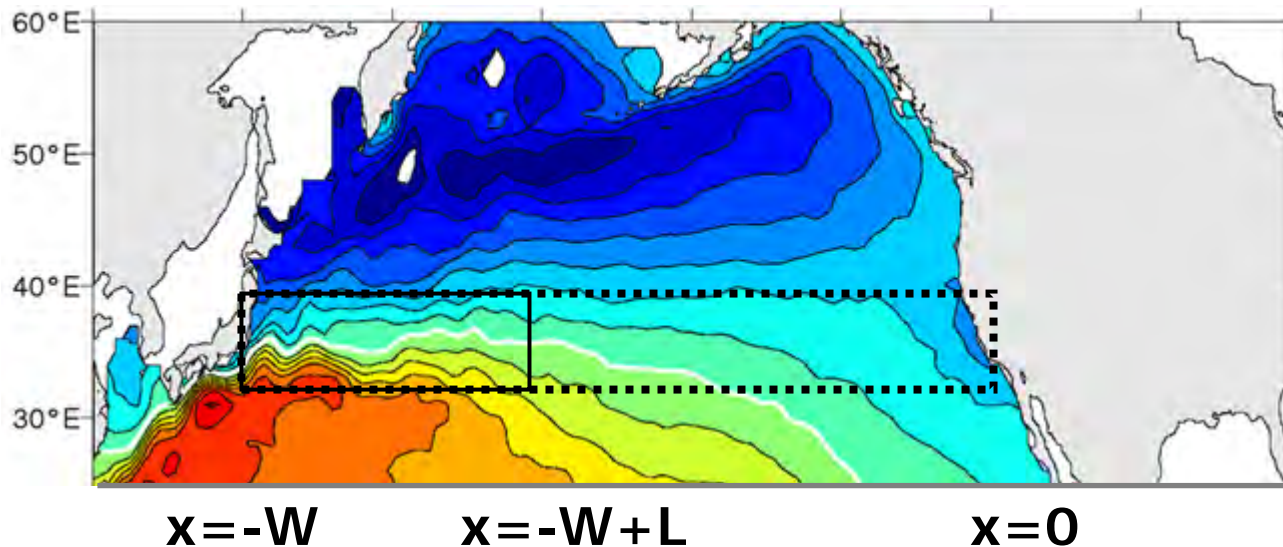
$$\frac{\partial h(x, t)}{\partial t} - c_R \frac{\partial h(x, t)}{\partial x} = -\frac{g' \text{curl} \tau}{\rho_0 g f} \quad (1)$$

$$\frac{\partial T(t)}{\partial t} = a \overline{h(t)} - \lambda T(t) + q(t) \quad (2)$$

$$-\frac{g' \text{curl} \tau}{\rho_0 g f} = \sum_{n=1}^2 \sin\left(\frac{n\pi x}{W}\right) w_n(t) + b \sin\left(\frac{2\pi x}{W}\right) T(t) \quad (3)$$

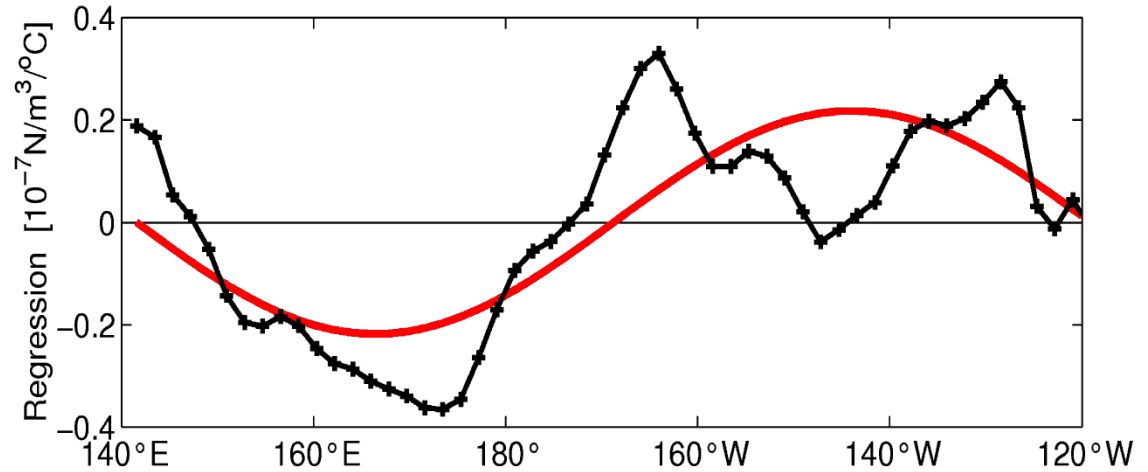
intrinsic

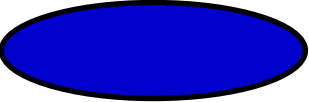
feedback



Lagged regression between KE SSTA and NP curl-tau field

- NCEP reanalysis data (1950-2008)
- ENSO signals (Nino 3.4) regressed out
- Different curl patterns with +/- lag



-  $p' > 0$; curl-tau < 0
-  $p' < 0$; curl-tau > 0

(b) $m=3$: SST(DJF) vs. curl (MAM)

